PII: S1350-9462(00)00013-6

Assessing Retinal Function with the Multifocal Technique

Donald C. Hood*
Department of Psychology, Columbia University, 116th and Broadway, New York, NY 10027-7004, USA

CONTENTS

.

*Tel.: +1-212-854-4587; Fax: +1-212-854-3609; E-mail: don@psych.columbia.edu

Progress in Retinal and Eye Research Vol. 19, No. 5, pp. 607 to 646, 2000

Printed in Great Britain
1350-9462/00/$ - see front matter

Abstract—With the multifocal technique, as developed by Erich Sutter and colleagues, scores of focal electroretinogram (ERG) responses can be obtained in a matter of minutes. Although this technique is relatively new, it has already provided insights into the mechanisms of retinal disease. However, because it is new, there also remain questions about how it works and what it measures. This chapter considers some of these insights and some of these questions. The first part (Section 2) describes how the multifocal ERG (mERG) is recorded and considers its relationship to the full-field ERG. The mERG responses are shown to be from relatively local regions of the retina and are comprised of the same components as the full-field ERG. The diagnostic advantage of the mERG as compared to the full-field ERG is also illustrated. In Section 3, the effects of damage to different cell layers of the retina are shown to affect the mERG differently, and these changes are summarized within a conceptual framework. It is argued, for example, that when diseases of the receptor outer segment, like retinitis pigmentosa, result in small, depressed mERG responses, then the damage is, as expected, at the outer segment. However, when these diseases result in mERG responses that are reasonably large but very delayed, then the damage is beyond the outer segment, probably in the outer plexiform layer. The implicit time of the mERG, not amplitude, is the more sensitive measure of damage in degenerative diseases of the receptors. On the other hand, diseases, like glaucoma, which act on the ganglion axon, do not result in easily identified changes to the mERG unless inner retinal damage is involved as well. Inner retinal damage changes the waveform of the mERG and decreases the naso-temporal variation normally observed. Finally, diseases, like diabetes, that act on more than one layer of the retina can have a range of effects. In Section 4, recent work with the monkey mERG is reviewed, with emphasis on the relevance to human diseases. For example, blocking the sodium-based action potentials produced by ganglion and amacrine cells eliminates the naso-temporal variation in the monkey mERG and these altered mERG responses resemble those from some patients with diabetes or glaucoma. Finally, in Section 5 the second-order kernel is described. The presence of a second-order kernel has important implications for understanding the shape of the mERG response (first-order kernel). Full-field simulations of the mERG paradigm illustrate that the first-order kernel is comprised of responses with different waveforms. Further, it is argued that the nonlinear, adaptive mechanisms that produce the second-order kernel are involved in shaping the time course of the response. Patients with large, but abnormally delayed mERG responses (first-order kernel), do not have a detectable second-order kernel. It is speculated that a markedly diminished second-order kernel is diagnostic of outer plexiform layer damage, not inner plexiform layer damage as is commonly assumed.

1. INTRODUCTION

The electroretinogram (ERG) is a mass potential, the result of the summed electrical activity of the cells of the retina. Before the advent of single-cell recording, our understanding of retinal physiology was based upon the ERG (Granit, 1947; Riggs, 1965). Although, for a time, the ERG fell out of favor in basic research, it remained a valuable tool for the clinician because it could be

readily measured from the human eye. Over the last ten years or so, there has been renewed interest in the ERG as a technique for studying both the physiology of the normal human retina, as well as retinal function affected by disease. This renewed interest can be traced in part to a better understanding of the cellular basis of the major components of the primate ERG. In the case of the scotopic or rod-driven ERG, techniques are now available for assessing the activity of the human rod receptor and bipolar cells and these techniques have been applied to the study of the normal and abnormal human retina (reviewed in Hood and Birch, 1996a, 1997; Birch *et al*., 1995; Robson and Frishman, 1999).

The photopic or cone-driven ERG is less well understood, in part because its cellular components are more complicated. Both on- and off-bipolars contribute to the cone ERG, as do sizeable high frequency components (the so-called OPs or oscillatory potentials). Second, unlike the rod system, the retinal cone system is spatially heterogeneous. The number and nature of the cells change dramatically with retinal eccentricity, from the fovea to the periphery. The local contribution to the full-field ERG thus differs for different retinal regions. As a result, the full-field, cone ERG is a mix of responses from a diverse array of cells and from different retinal regions. This presents a problem for studying the activity of the normal human retina with the full-field ERG. Further, many diseases of the cone system affect local regions of the retina. The multifocal ERG (mERG) technique was developed by Sutter and colleagues to deal with these problems (Sutter, 1991; Sutter and Tran, 1992).

The multifocal technique can produce 100 or more focal responses from the cone-driven retina in 7 min of recording or less. Although this technique is relatively new, it has already provided interesting insights into the mechanisms of retinal disease. However, because the multifocal technique is new, there remain some questions about how it works and what it measures. Some of these insights and some of these questions are dealt with here.

2. THE HUMAN MERG: SOME BASICS

2.1. How is it recorded?

The subject fixates on the center of a CRT display containing an array of hexagons that increase in size with distance from the center (Fig. 1). Typically, the sizes of the hexagons are scaled, inversely with the gradient of cone receptor density, so as to produce focal responses of approximately equal amplitude in control subjects (Sutter and Tran, 1992). The display usually contains either 61 or 103 hexagons, although 241 hexagons have been used in a few experiments to obtain higher spatial resolution. The retinal size of the display varies across laboratories, but is nearly always less than 35° in radius and most commonly subtends 21–25° in radius, similar to the area tested by standard clinical visual fields with automated perimetry. Although a wide range of stimulus intensities have been employed, in the most commonly employed display the luminance of the white hexagon is set to 200 cd/m^2 and the black hexagon to the lowest value available.[1] This produces a contrast between about 85% and 98% depending upon the monitor. In all cases, this is nominally referred to as a display with a mean luminance of 100 cd/m^2. As with full-field ERG recording, the pupil is usually, but not always, dilated.

During stimulation, the display appears to flicker because each hexagon goes through a pseudo-random sequence (the m-sequence) of black and white presentations. Each hexagon has a probability of 0.5 of being white or black on each frame change. Typically, the frame is changed every 13.33 ms (a frame rate of 75 Hz). However, the actual duration of the incremental light producing a white hexagon depends upon the phosphor of the monitor and is only a few milliseconds in duration. The pseudo-random stimulation is illustrated in Fig. 1. In Fig. 1(A), the upper, double-headed arrow points to a hexagon that is white at the time indicated as 0 and the lower one to a hexagon that is black at time

[1]As in the case of the full-field ERG, chromatic and pattern reversal stimuli have been tried. This work is beyond the scope of this review.

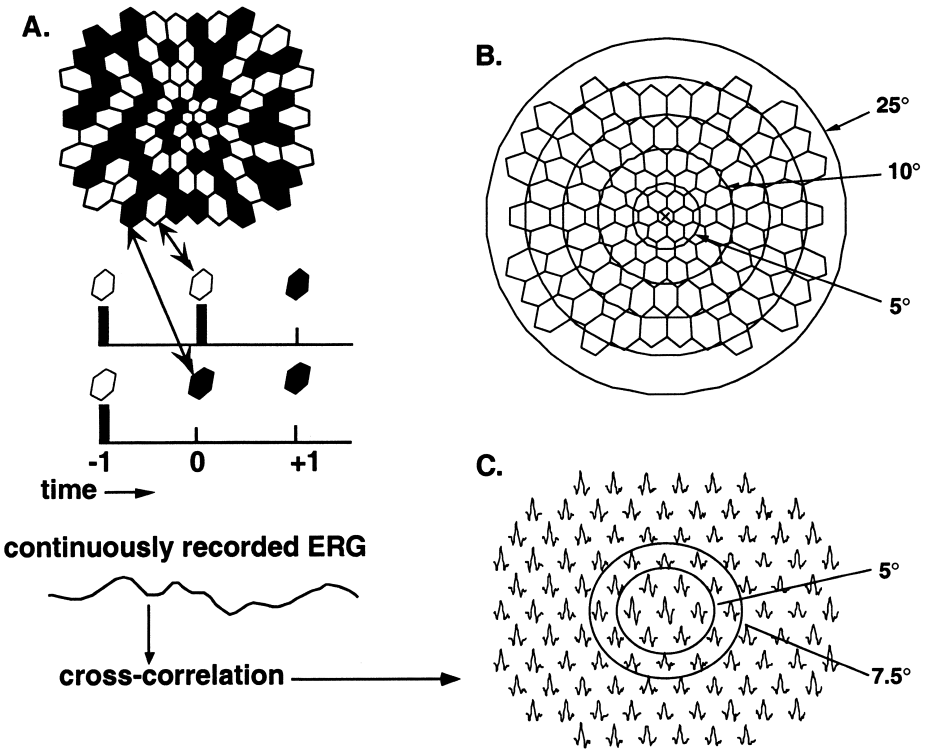

Fig. 1. The mERG is recorded to an array of black and white hexagons (A) that are scaled with distance from the fixation point (B). The hexagons go through a pseudo-random sequence of black and white as the frame changes (B). After about 7 min of recording, a cross-correlation technique produces multiple ERG records, one associated with each of the hexagons (C).

0. On the previous frame (i.e. 13.3 ms earlier), both hexagons were white. In this example, both hexagons are black during the next frame, at time +1. Every hexagon in the array is stimulated with the same m-sequence of white and black presentations, but each hexagon starts at a different point in the sequence. This allows the responses to be derived with a fast algorithm (Sutter, 1991).

While the subject views this display, a single continuous ERG record is obtained using the same electrodes and amplifiers employed for standard ERG recording. Typically this continuous record is about 7 min, but can be under 4 min for clinical screening, and is obtained in 15 or 30 s segments so as to make it easier for the subject to suppress eye movements and blinks. From the single continuous record, the 103 (or 61) focal responses are derived, with each response tied to stimulation in a particular hexagon. Figure 1 shows the responses for a display with a mean luminance of 100 cd/m^2, along with the array of 103 hexagons. With the standard stimulus display of 103 scaled hexagons, the central seven responses are associated with hexagons falling within the central 5° (compare panels B and C). [By convention, the term "central x°" refers to the radius of the field with the fovea as the center.] Technically, these responses are the first-order kernels of the cross correlation between the stimulation sequence and the continuously recorded ERG. [Further details about this technique can be found below and in the literature (Sutter, 1991; Sutter and Tran, 1992; Wu and Sutter, 1995; Bearse and Sutter, 1996; Hood *et al.*, 1997; Keating *et al.*, 2000).]

2.2. What is the first-order kernel?

The mERG responses in Fig. 1(C) are first-

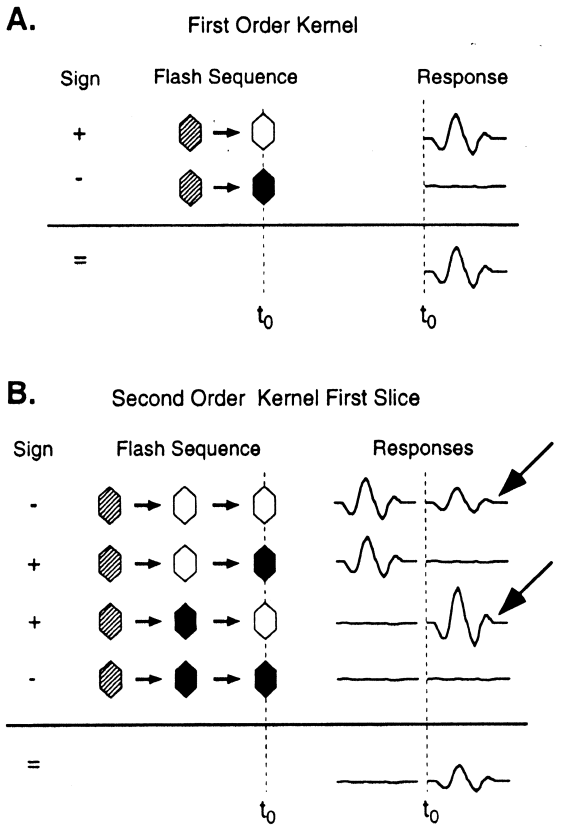

Fig. 2. A schematic illustrating the derivation of the first- and second-order kernels of the mERG. Open hexagons indicate a flash occurred on that frame change; the black hexagons indicate a flash did not occur; and the hexagons with the diagonal lines indicate a frame that could have had either a flash or no flash. Modified and reproduced by permission from Sutter and Bearse (1999).

order kernels. Figure 2(A), from Sutter and Bearse (1999), schematizes the derivation of the first-order kernel, for a given hexagon. Mathematically, it can be obtained by adding all the records following the presentation of a flash in that hexagon (i.e. the presentation of a white hexagon), and subtracting all the records following a dark frame (black hexagon). In a sense, by adding the records immediately following the presentation of a flash in a given hexagon and subtracting the records immediately following a "non-presentation", the response to that hexagon is built up, while the responses associated with all other hexagons are eliminated.

There are two common misconceptions about the first-order kernel. First, because its amplitude varies approximately with cone density (Sutter and Tran, 1992), some believe that it is the response of the cone receptors. However, the density of other retinal cells, in particular the bipolar cell, is also roughly proportional to cone density. In fact, we will see below that very little of the mERG response is generated by the cone receptor per se, but rather is dominated by the responses of the bipolar cells. Second, this first-order response is sometimes mistakenly described as the impulse response of the retina at a particular location. Technically, the first-order response is the "impulse response" only if the system is linear. However, non-linearities exist and account for the difference between the appearance of the mERG and the full-field ERG; these nonlinearities are discussed in Section 5 where the second-order kernel is described.

2.3. A comparison to the full-field ERG

The waveform of the mERG response does not look like a typical photopic ERG. Thus, the question naturally arises about the relationship of the waveform of the mERG to that of the full-field ERG. For comparison to the full-field ERG, the 103 focal ERGs from Fig. 1(C) were summed to produce the response in Fig. 3(A). We will call this the "summed mERG". A full-field ERG from the same subject is shown in Fig. 3(B) for comparison; it is scaled to have about the same peak-to-trough amplitude. The initial negative portion of the full-field ERG and the summed mERG appear similar, but the positive components do not. The peak of the summed mERG occurs at an earlier time and its waveform lacks the multiple positive components seen in the full-field ERG. Although, for Fig. 3, a single white hexagon (one frame) for the mERG (panel A) has about the same energy (3 cd-s/m^2) as the incremental full-field flash (4 cd-s/m^2) for the full-field ERG (panels B and C), the two techniques differ in other ways including the pass band of the amplifier, the stimuli employed and the data analysis performed.

The pass band of the amplifier is not a major factor. For the mERG, the amplifier cutoffs were

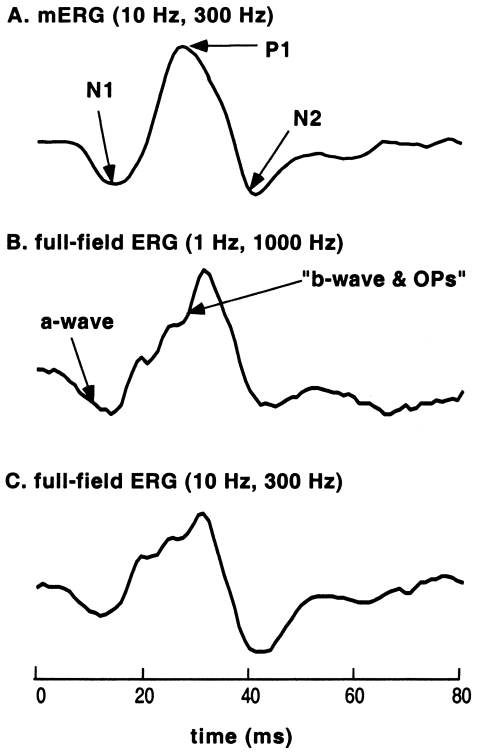

Fig. 3. The summed mERG from Fig. 1(C), recorded with amplifier cutoffs of 10 and 300 Hz (A). For comparison, full-field ERGs to about the same flash intensity were recorded with cutoffs of 1 and 1000 Hz (B) or 10 and 300 Hz (C). Recorded at NYU Medical Center with Drs. Karen Holopigian and Bill Seiple.

set at 10 and 300 Hz, while for the full-field ERG in Fig. 3(B), these cutoffs were 1 and 1000 Hz. Figure 3(C) shows a full-field ERG response for the amplifier settings employed in the mERG recordings, 10 and 300 Hz. The waveform of the full-field ERG is affected, but remains distinct from that of the mERG. The 10 Hz filter setting is employed in mERG recordings because it removes some of the effects of small eye movements. Small eye movements can saturate the amplifier and substantially lengthen the time needed to obtain viable recordings. Responses obtained with the 10 Hz filter setting will have shorter implicit times of P1 than if lower (e.g. 1 or 3 Hz) settings are employed. However, in most cases, the 10 Hz setting will not affect the interpretation of the mERG. On the other hand, Keating *et al.* (1997) have pointed out that using a cutoff of 10 Hz can distort responses that are sustained, such as the negative responses occasionally seen in patients with retinal vascular problems and can lead to a misinterpretation of the changes in the mERG.

Given the various differences between the full-field and multifocal paradigms, it is not surprising that the waveforms of the responses differ. In the mERG paradigm there is no steady background present, the flashes are closely spaced in time (appearing on average at half the frame rate, or every 26.7 ms), and the response is derived as the first-order linear correlation. On the other hand, for the full-field cone ERG, a background is present, at least 1 s is allowed between flashes for the cone system to recover, and individual responses are averaged directly from the continuous record. It turns out that the most important difference between these paradigms is the time between flashes.

The mERG paradigm can be modified as in Fig. 4(A), so as to make it more like the full-field paradigm (Hood *et al.*, 1997). Here the sequence of multifocal flashes is slowed down and the hexagons appear as increments upon a background; the m-sequence includes seven frames (106 ms) of this background. Thus, individual flashes can be no closer than 106 ms and are separated on an average by 212 ms. This m-sequence will be referred to as the 7F condition while the standard condition will be called 0F. With the 7F condition, there is good agreement between the full-field ERG and mERG waveforms (Fig. 4(B)). Of course, the summed mERG responses are smaller because the display does not cover the full field. In Fig. 4(B), the summed mERG responses have been scaled by a factor of 4, about the amount expected due to the difference in proportion of cone receptors covered. [According to the anatomical data of Curcio *et al.* (1990), the central 25°, approximately the area covered by the multifocal array, contains about 23% of the human cone receptors.] Except for the highest intensity, the agreement is remarkably good. Even at the highest intensity, the mERG waveform obtained with the 7F sequence exhibits the general shape of the full-field ERG and differs markedly from the waveform for the 0F condition.

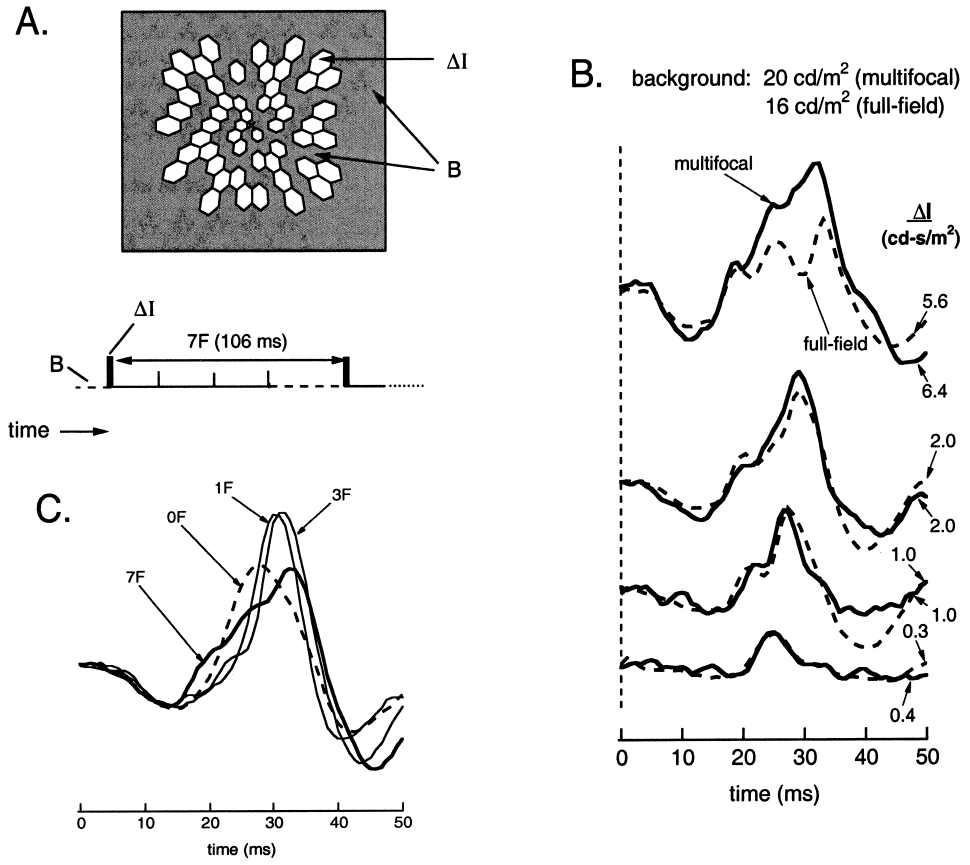

Fig. 4. The mERG m-sequence is modified to include seven frames of a low-intensity background (A). This paradigm produces mERG waveforms that resemble full-field ERG waveforms for comparable conditions (B). As the number of background frames is decreased, the waveform of the mERG changes (C). Modified from figures in Hood *et al.* (1997).

The critical difference between the two paradigms is the temporal density of the flashes. As the number of background frames is increased, the summed mERG approaches the waveform of the full-field ERG (Fig. 4(C)). The N1 ("a-wave") is largely unaffected by the number of blank frames, but P1 goes from a multi-peaked wave (a "b-wave" and "OPs") for the 7F condition to a single peak for the 0F condition. The fast 0F sequence is producing a high contrast stimulus at a high adaptation level. In sum, the waveform for the 0F condition does not look like a full-field ERG because the stimulus conditions (particularly the rate of stimulation) are not the same. Some of the factors involved in producing the mERG waveform are considered further in Section 5.

2.4. Are the mERG responses "little" ERGs?

The answer to the question "Are these little ERGs?" is a qualified "yes", and the qualifications depend upon the sequence of stimulation. If seven or more frames of the background are inserted between hexagon presentations, then these responses are little ERGs, with waveforms that appear reasonably close to responses obtained with more traditional focal stimulation (Miyake, 1990). In the case of the standard 0F condition, the answer appears to be also "yes", in the sense that N1 is comprised of the same components as the a-wave of the full-field ERG and P1 is comprised of the same components as the positive waves (b-wave and OPs). However, we will see below (Section 5.5) that the waveform

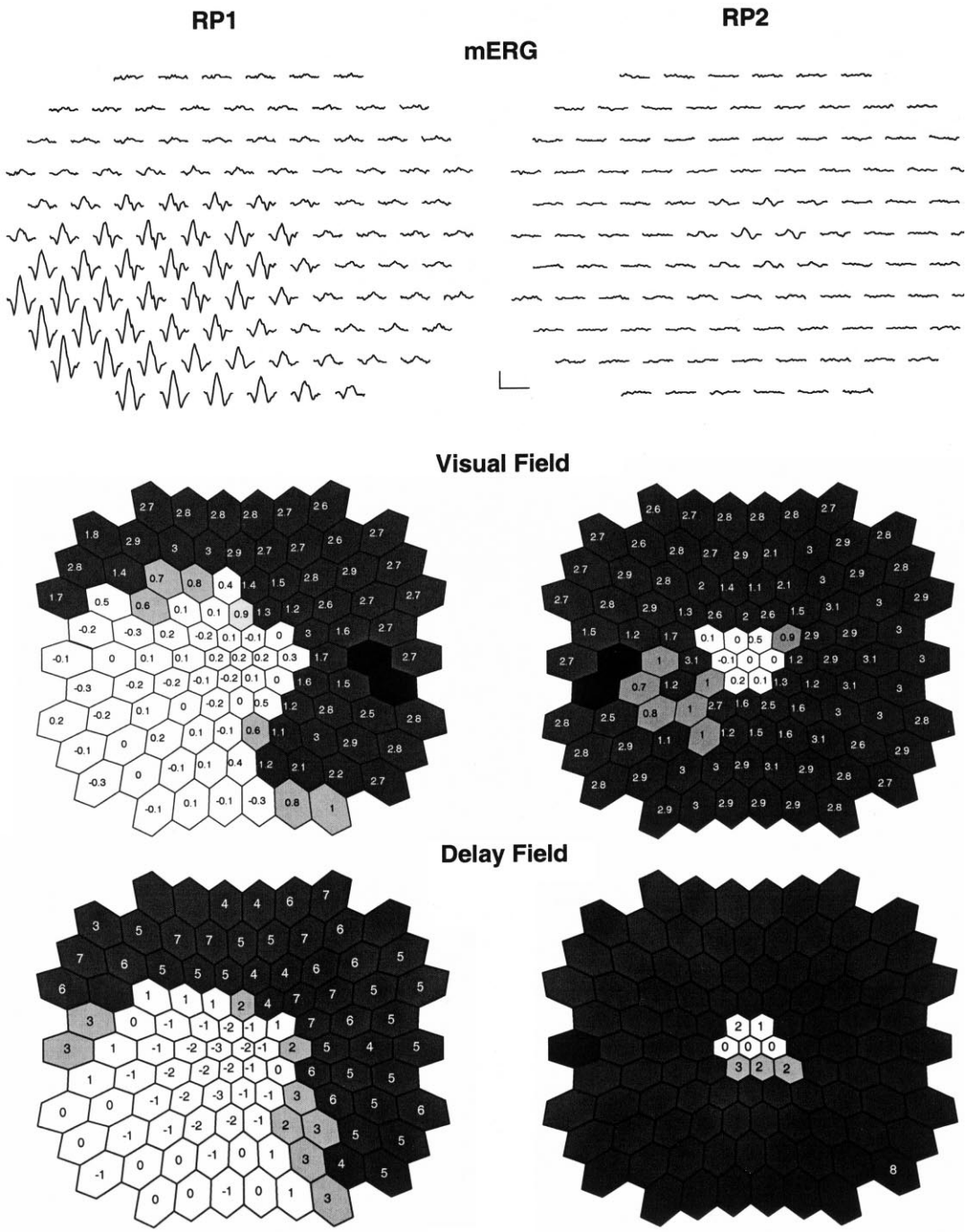

Fig. 5. The mERG records for two patients with RP (top panel). The calibration bars indicate 200 nV and 60 ms. Patient RP1 is the same person as P1 in Hood *et al.* (1998a), but these recordings were made over three years later. Patient RP2 records were obtained in Dr. David Birch's laboratory at The Retina Foundation of the Southwest in Dallas, TX. This patient had a visual acuity of 20/30. The visual fields (middle panels) for both patients, obtained by modifying the Humphrey program, show good correspondence to the mERG responses. The delays in the implicit time of the positive peak (lower panels) are expressed relative to the values for a group of control subjects.

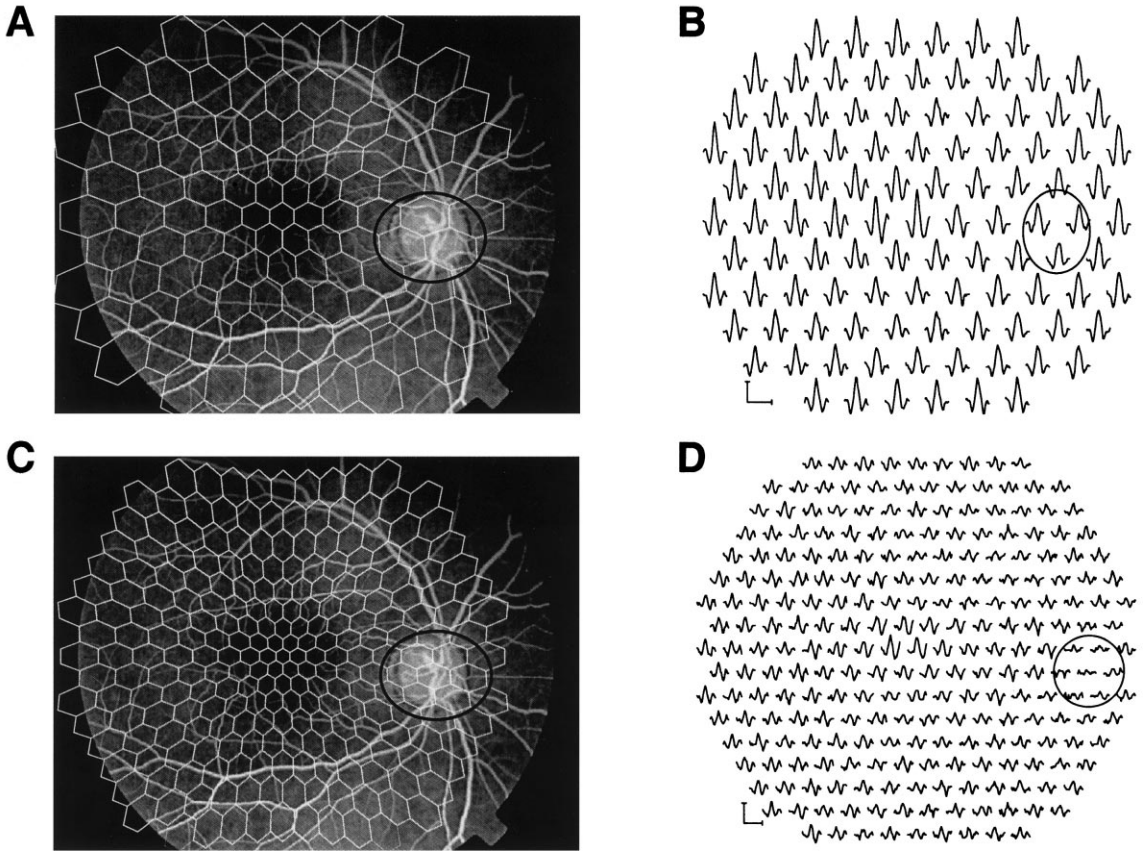

Fig. 6. The fundus photograph of a right eye, flipped to correspond to the visual field, is shown with the 103 (A) and 241 (C) mERG arrays. Records (B) and (D) from two control subjects are shown; the circled responses are from regions near the blind spot and correspond to the circled hexagons in (A) and (C). The calibration bars indicate 200 nV and 60 ms. These records can be found among the normal controls (B49-CR and sj.241) in the VERIS 4.x software from EDI (San Mateo, CA) and are presented here with permission from Dr. E. Sutter.

of the first-order response does not exactly correspond to the response to any single flash including the flashes in the m-sequence.

2.5. How local are these focal responses?

A priori, the spatial resolution of the multifocal technique must be reduced, to some extent, by stray light. Further, neural networks that extend beyond the area of a particular hexagon will affect the extent to which an individual response can be tied to the activity of a local retinal region. It appears that, for most purposes, both considerations are relatively unimportant. Evidence for this conclusion comes from mERG responses obtained from patients with damage to the receptors (see Fig. 5) as well as from studies on local light adaptation of the normal retina (Bearse and Sutter, 1996). Retinitis pigmentosa (RP) results in widespread receptor damage. The mERGs from two patients with RP are shown in Fig. 5 (top panel) along with their behaviorally determined visual fields (middle panels). For the visual fields, the test spot of a Humphrey perimeter was presented in the center of each hexagon. The white regions indicate normal sensitivity and the black regions indicate that sensitivity is more than 4 s.d. (about 10 dB or 1.0 log unit) from normal. In both patients, the amplitude of the mERG response is very small immediately outside the region of the field with near-normal sensitivity. The mERG responses

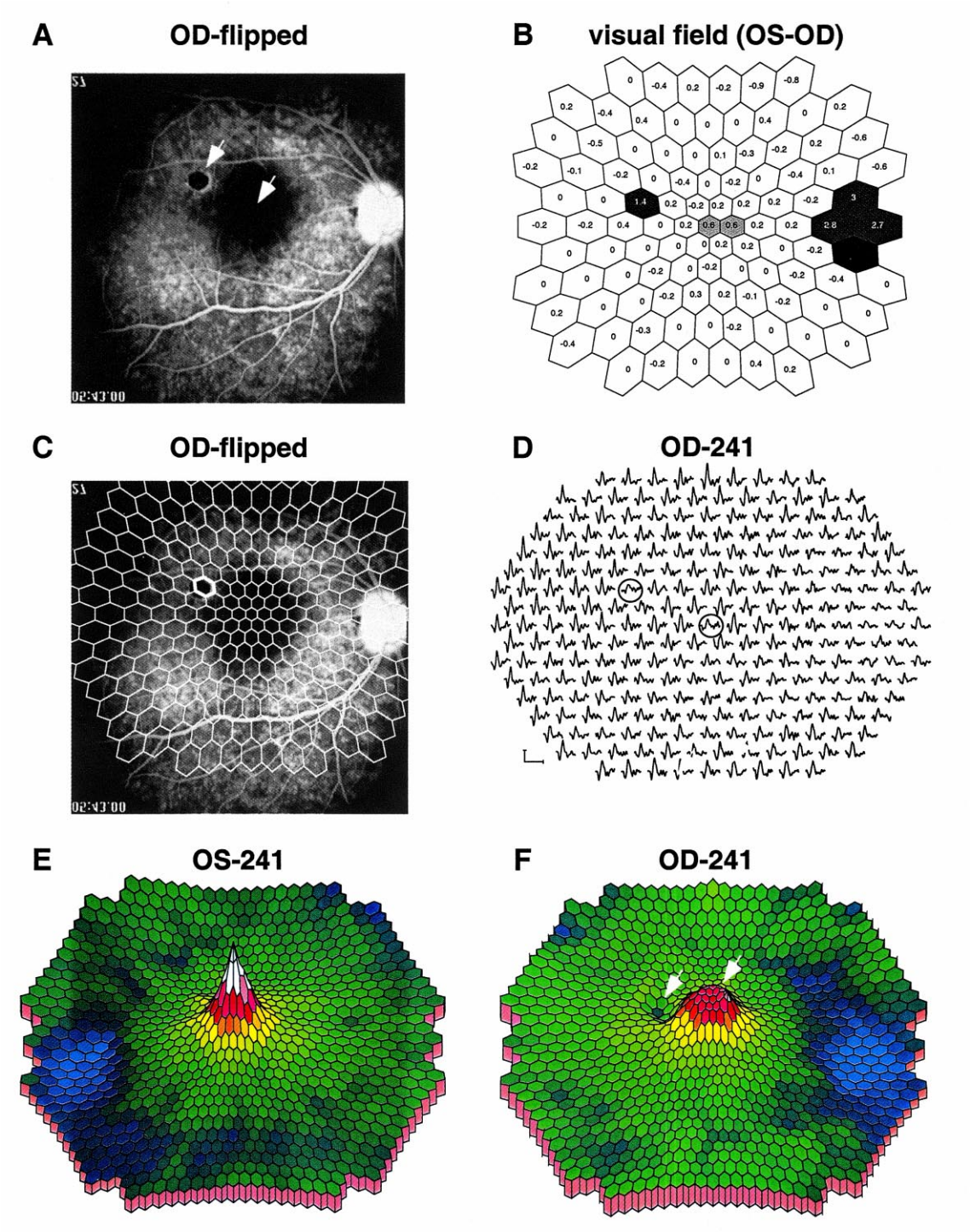

Fig. 7. (*Caption opposite*).

from patients such as these argue that the multifocal responses are reasonably local.

On the other hand, the mERG responses must be influenced by light scatter, but we do not know by how much. The lack of a clear blind spot in control records has been taken by some to indicate a considerable influence of stray light. However, a closer look at this evidence argues for a reasonably local mERG response. With the 103 element display, there is no guarantee that a hexagon will fall entirely within the optic disc (see Fig. 6(A)). [The records in Fig. 6(B) and (C) are from a right eye and are shown referenced to the visual field. The fundus view has been flipped to correspond to the mERG.] With a display of 241 elements, at least one hexagon should fall entirely within the disc if steady fixation is maintained (Fig. 6(C)). It is now easier to see the diminished response due to the blind spot (Fig. 6(D)), in spite of the fact that the reflective nature of the blind spot should accentuate the effects of scattered light. The exact contributions of eye movements and scattered light to the responses in the region of the blind spot remain to be determined. Lowering the mean luminance of the display, for example, makes the blind spot more obvious in the mERG responses (see asterisk in Fig. 12).

Although we can conclude that the local effects of disease and, within reason, local retinal circuitry can be studied with the mERG, the spatial resolution of the technique has yet to be precisely determined. The records in Fig. 7 suggest that it can detect a scotoma of less than 4°. This patient had normal vision in her left eye and two very local problems in her right. Modified 103 Humphrey fields like those in Fig. 5 (middle panels) were obtained for each eye. The visual field in Fig. 7(B) was obtained by subtracting the visual field values for the affected right eye from those for her normal left eye. The field shows two localized field losses in her right eye, as well as an enlarged blind spot. There is a central loss of 0.6 log unit (6 dB) and a 1.4 log unit (14 dB) loss about 7° from fixation. The latter deficit appears as a scar (left arrow in Fig. 7(A)) that appeared about 7 years earlier and was diagnosed at the time as the result of toxoplasmosis. [This pericentral deficit does not appear on the patient's Humphrey 24-2 field where the test locations are separated by 6°, but does appear as a deep scotoma on her Humphrey 10-2 field where the test locations are separated by 2°.] These relatively localized field losses can be seen in her mERG responses (circled records in Fig. 7(D)) and these deficits, along with the enlarged blind spot, can be visualized in the 3D plots of local response density (Fig. 7(F)).

2.6. Studying and diagnosing the abnormal retina

In diseases of the outer retina, the mERG provides spatial information not readily available in the full-field ERG. This is apparent in the comparison of full-field ERG to mERG responses in Fig. 8. In this patient (RP2 from Fig. 5), there is less than a 300 nV response to the full-field 30 Hz stimulus, and the full-field ERG response is not detectable to the other stimuli that is part of the standard (ISCEV) clinical protocol (see also case 1 in Kondo *et al.*, 1995). It is clear from the mERG records that any detectable full field signal is coming almost entirely from the central 5°. In general, the full-field 30 Hz flicker responses from patients with RP are summed from multiple regions in different states of disease. These different states are hidden in the full-field ERG but are readily seen with the mERG (see Hood *et al.*, 1998a and Fig. 16 below).

The mERG is being used routinely in some clinics to help differentiate diseases that affect the outer retina from those that affect the ganglion

Fig. 7. The fundus photograph (A) of the right eye, flipped to correspond to the visual field, of a patient presenting with a sudden loss of visual acuity (20/70). The pericentral scar indicated by the arrow (in (A)) appeared about 7 years earlier and was diagnosed at the time as being due to toxoplasmosis. The visual field (modified 103 Humphrey as in Fig. 5, middle panel) of the patient's right eye (B) is the difference between the fields from her two eyes; it shows localized central and pericentral losses as well as an enlarged blind spot. Her mERG responses (D) to the 241 array show local changes corresponding to the changes in her field. The calibration bars (in D) indicate 100 nV and 80 ms. These changes can also be seen in the 3D plots of response density (E) and (F) produced by the VERIS software. This is a patient of Dr. Jeffrey Odel and these records are shown with his permission.

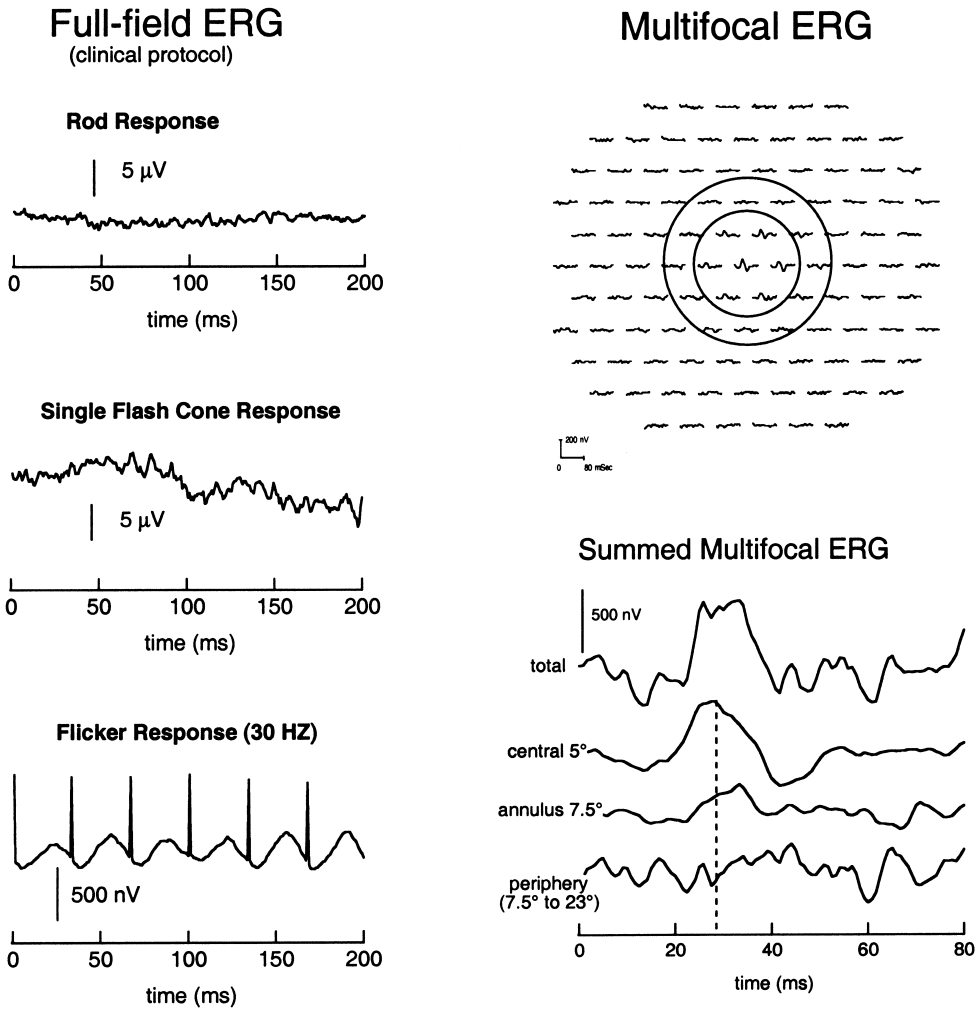

Fig. 8. The full-field ERG records from a standard clinical protocol (left column) and the mERG records (right column) are shown for patient RP2 (from Fig. 5). These records were obtained in Dr. David Birch's laboratory at The Retina Foundation of the Southwest in Dallas, TX.

cell or optic nerve. The patient whose records are shown in Fig. 9 was initially thought to have an optic nerve problem because her acuity was reduced and her full-field ERG was normal. Her mERG responses show depressed amplitudes in the center and these central responses have small implicit time delays. This pattern resembles that reported by Kretschmann *et al.* (1998a,b) for patients with early Stargardt's. This diagnosis was subsequently confirmed on the basis of fundus pictures.

Finally, the mERG is being used to follow the effects of clinical intervention. For example, patients have been followed before and after treatment for retinal detachment. It takes over a month or more for the mERG to recover, and the mERG changes correlate with the recovery of visual acuity and visual field sensitivity (Moore *et al.*, 1999) although the mERG may be more disturbed than expected from the visual fields (Sasoh *et al.*, 1998). Greenstein and her colleagues have followed patients with macular edema, secondary to diabetic retinopathy, before and after laser treatment (Greenstein *et al.*, 2000)

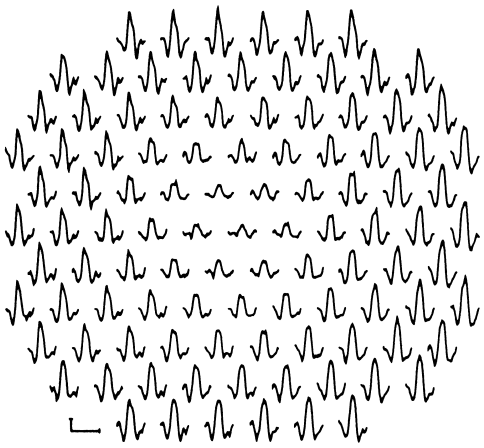

Fig. 9. The mERG responses from the right eye of a patient with Stargardt's macular dystrophy (SMD). The calibration bars indicate 125 nV and 60 ms. This is a patient of Drs. Miles Behrens, Jeffrey Odel and Ron Carr; these mERGs were recorded by Dr. Karen Holopigian, and are shown with permission from all concerned.

and, Si *et al*. (1999) have followed patients before and after macular hole surgery. It is likely that new uses of the mERG technique will be found as new interventions are developed. It should be particularly useful in situations where localized changes are expected such as with experimental, retinal transplant procedures (Radtke *et al*., 1999) and local drug injections. The normative values (Parks *et al*., 1997; Nagatomo *et al*., 1998; Verdon and Haegerstrom-Portnoy, 1998), the repeat reliability measures (Parks *et al*., 1997) and the techniques for differentiating signals from noise (Hood and Li, 1997) needed for clinical trials are starting to appear.

2.7. Studying local responses from the normal retina

2.7.1. *The full-field, cone ERG is comprised of different waveforms*

The spatial aspect of the mERG offers an advantage for studying the normal retina as well. Earlier studies of focal cone ERGs indicated that the waveform of the ERG varies with retinal location (e.g. Miyake *et al*., 1989; Miyake, 1990). These variations can be readily seen and studied with the mERG if the m-sequence is slowed (Wu and Sutter, 1995; Hood *et al*., 1997). The waveform of the summed mERG to a slowed (7F) sequence resembles the waveform of the full-field ERG (see Fig. 4). Interestingly, this mERG elicited with the 7F sequence exhibits wide variation in waveform with retinal location, as shown in Fig. 10. The first two columns are responses to a 7F sequence expressed as response density (voltage/unit area) and as the summed response (total voltage). The top traces are the responses to the central hexagon and successive traces are the responses to the five concentric rings of hexagons. Because of the high density of cone receptors (top insert) in the fovea and the high density of post-receptor cells to which they connect, the response to the central hexagon has the largest response density. Notice, however, that the column of summed responses indicates that the relative contribution of the center to the overall summed mERG will be negligible. Clearly the peripheral responses will dominate both the summed mERG and the full-field ERG. Further, the mERG waveform changes with eccentricity; thus the waveform of the summed mERG or the full-field ERG will not be representative of any particular location.

In addition to variations with eccentricity, the waveforms of the mERG to the 7F sequence also show both nasol-temporal and superior–inferior variations (see upper and left traces in Fig. 11). The responses from the parafoveal regions contain more OP activity, with the OPs in the temporal retina being more prominent than those in the nasal retina (Wu and Sutter, 1995; Miyake *et al*., 1989; Miyake, 1990). Studies with monkeys are beginning to help us understand the relationship of the variations in these local responses to cells of the retina (Hood *et al*., 2000a; see also Section 4).

2.7.2. *The standard mERG varies with eccentricity and luminance*

In contrast to the responses for the slowed sequence (7F), the responses for the fast sequence (0F) appear to show relatively little variation in waveform with retinal location. The changes in waveform from center to periphery (Fig. 10,

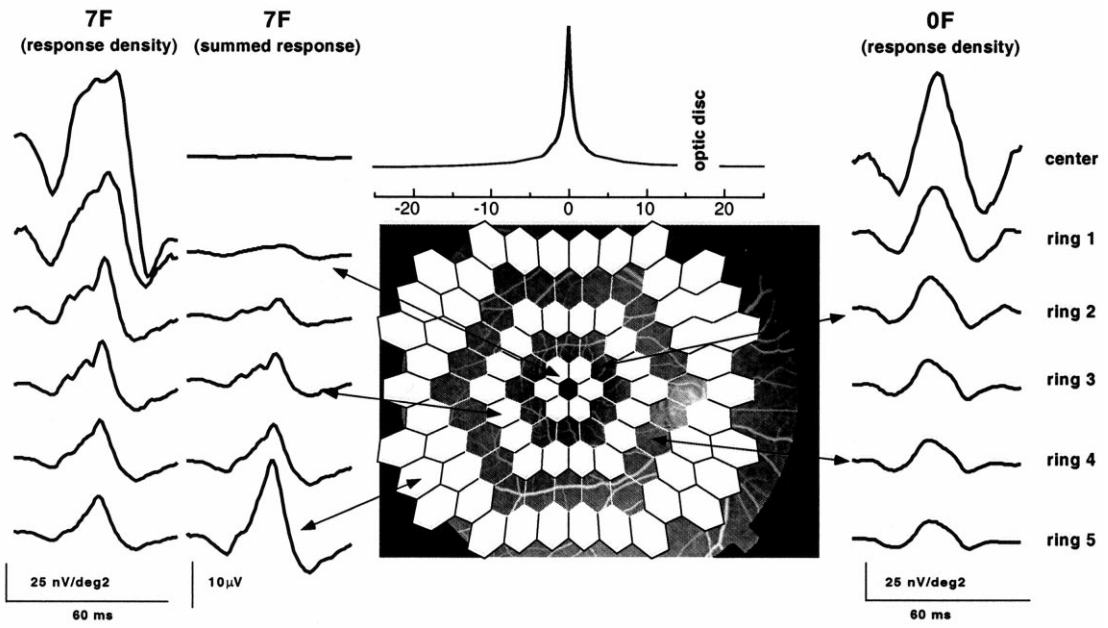

Fig. 10. The central response and the summed mERG responses around concentric rings are shown for a 7F and 0F m-sequence. The relative cone density, from Curcio *et al.* (1990), is shown above the fundus view of a right eye, flipped to correspond to the visual field.

rightmost column of responses) or across the horizontal or vertical midline (Fig. 11 — right and bottom) are subtle compared to the variation in waveform for the 7F sequence. However, there are differences in the 0F waveforms and these differences can be accentuated by lowering the mean luminance or changing the contrast. Figure 12 shows mERGs for two luminance levels recorded from the same subject on the same day. They are shown grouped by ring (rightmost column) as in Fig. 11 and by quadrant (see insert-middle column). With the most commonly used mean luminance of 100 cd/m^2, the implicit times of the more central responses are slightly longer than those of the peripheral responses (see dashed line in rightmost column), as initially reported by Sutter and Tran (1992). There are also naso-temporal differences in waveform as can be seen in the responses grouped by quadrant in the middle column of Fig. 12 and these differences are more apparent if the mean luminance is decreased (Fig. 12, lower panels). Below, we attribute the naso-temporal variations to inner retinal activity (Hood *et al.*, 1999a,b, 2000b). There are naso-temporal differences in the implicit time of P1 as well, as pointed out by Seeliger *et al.* (1998a). Differences in the timing of P1 can be quantified and displayed as a 3D plot (see Fig. 13). It is easy to detect the blind spot in these 3D plots: the implicit times are slower and the amplitudes are smaller than in the surrounding regions. In fact, Seeliger (personal communication) suggests that plots similar to these could be used to assess fixation accuracy. An easy way to see these timing differences in the array of responses is to restrict the temporal epoch to the first 35 ms (Fig. 14). Now the naso-temporal timing differences and blind spot timing differences can be visualized in the array of responses from the control subject (Fig. 14(A)).

Finally, why does the 7F sequence produce much larger regional variations in waveform than does the 0F sequence? The answer lies in the nonlinear processes that shape the waveform in the 0F sequence. This will be discussed in Section 5.

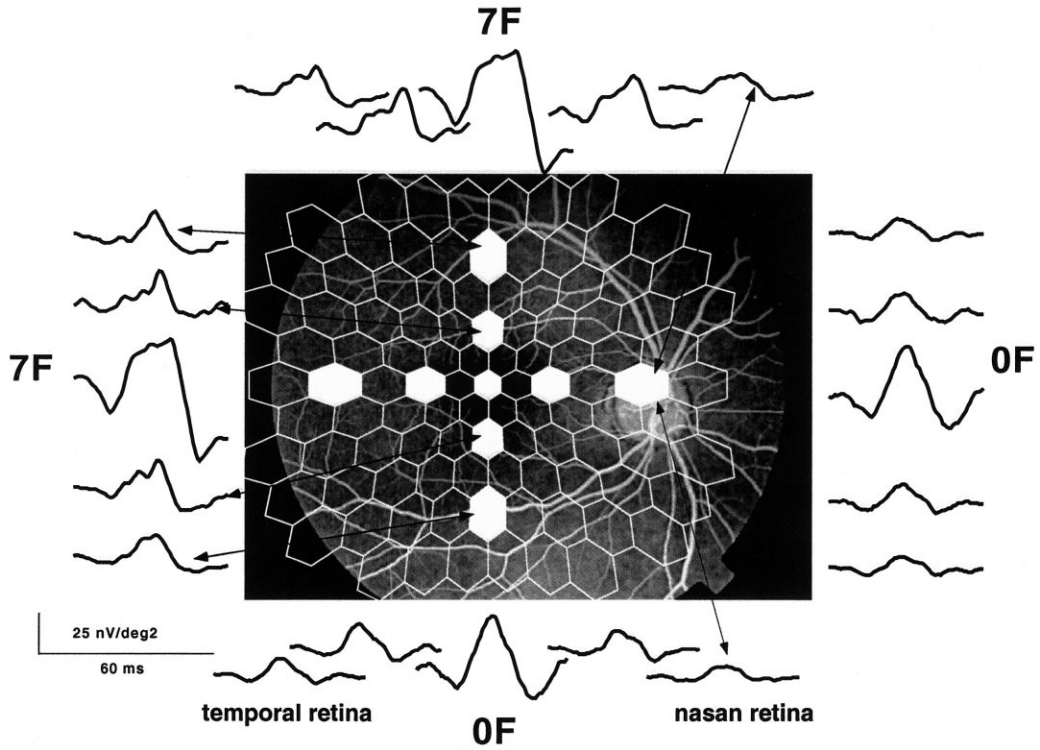

Fig. 11. The naso-temporal and superior–inferior variations of the mERG waveforms. More variation is seen with 7F (left and upper records) than with 0F (right and lower records).

3. THE MERG AND DISEASES OF THE RETINA

In the last few years, numerous articles have reported the effects of various diseases on the mERG. The attempt here is not to review this literature but to focus on what we have learned thus far about the relationship between the sites and mechanisms of retinal damage, on one hand, and changes in the mERG, on the other. To help summarize this information, a preliminary framework is proposed and summarized in Table 1.

Table 1. Sites and mechanisms of retinal damage and proposed changes in the mERG

Damage to	Mechanism	P1 ("b-wave") of mERG	
		Amplitude	Implicit time
1. Cone Receptor	Outer segment damage or cell loss	Smaller Smaller	Moderate delay Normal
2. Outer plexiform layer	Altered synaptic transmission	Can be normal or larger	Large delay
3A. On-Bipolar cells	Cell loss	Smaller	Moderate delay
3B.Off-Bipolar cells	Cell loss	Larger	Slightly faster?
4. Inner plexiform layer	Altered synaptic transmission or cell loss	Approx. normal (waveform changes)	Small delay (< 3 ms)
5. Ganglion cells	Cell loss	Approx. normal[a]	Approx. normal[a]

[a] May cause a loss of an ONHC.

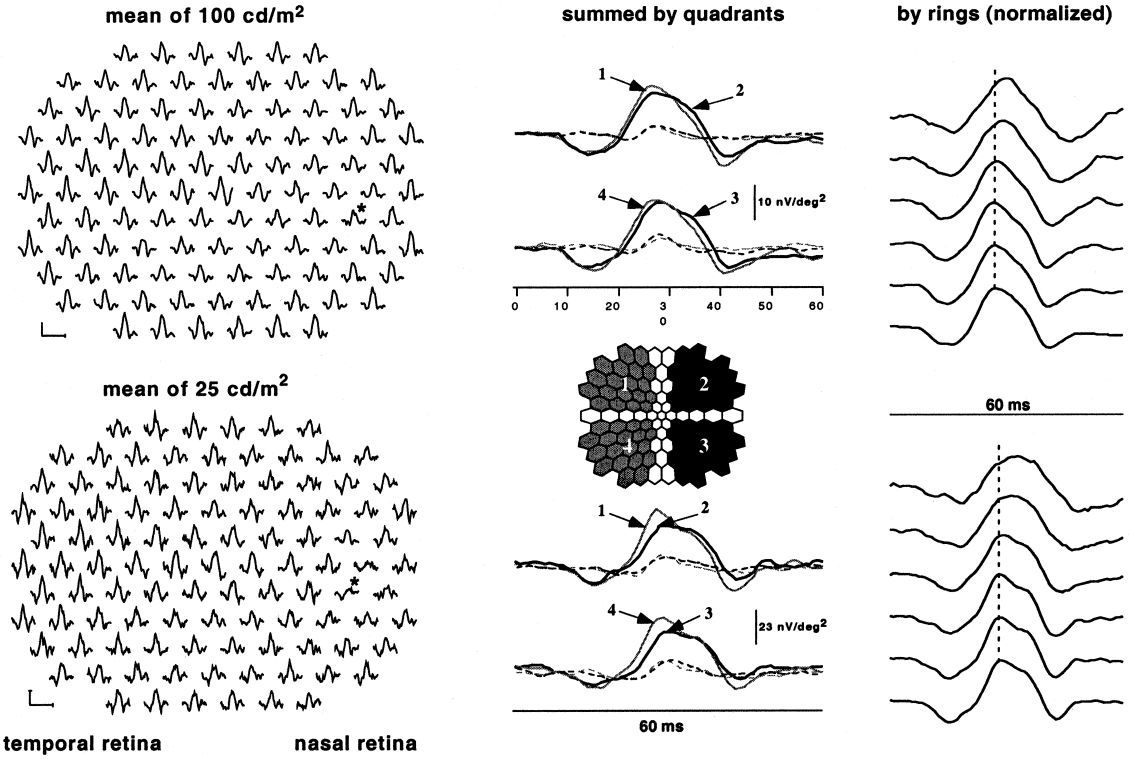

Fig. 12. The mERG responses (left column) for a mean luminance of 100 cd/m^2 (upper panels) and 25 cd/m^2 (lower panels). The horizontal calibration bars indicate 60 ms and the vertical bars 200 nV (100 cd/m^2) and 100 nV (25 cd/m^2). The blind spot (asterisk in arrays of left column) is more apparent at the lower luminance. Lowering the luminance also increases the naso-temporal variation in waveform (middle column) and the differences seen with eccentricity (right column). The arrows in the middle column indicate the summed response from the nasal (2 and 3) and temporal (1 and 4) retinal quadrants. The dashed curves in the middle column are second-order responses. The vertical dashed lines in the right column serve to illustrate the change in implicit time with eccentricity.

3.1. Damage to the receptors

3.1.1. *Retinitis pigmentosa: the importance of measuring both amplitude and implicit time*

A number of studies have looked at the mERG of patients with RP. The typical finding is that the amplitude is decreased, especially in the peripheral regions where visual fields are most affected (Kondo *et al.*, 1995; Hood and Li, 1997; Chan and Brown, 1998; Hood *et al.*, 1998a; Seeliger *et al.*, 1998a,b; Yoshii *et al.*, 1998). Reduced amplitude is associated with regions of markedly reduced visual field sensitivity (Fig. 5). It stands to reason that diseases that destroy the outer segments of the receptors will lead to a decrease in the amplitude of the mERG. However, in addition to the decreased amplitude, there are also delays in the implicit time. The small responses from regions of poor sensitivity, such as those in Fig. 5 for RP1, have longer implicit times. The timing of these small responses can be accurately measured (Hood and Li, 1997; Hood *et al.*, 1998a; Seeliger *et al.*, 1998a,b; Felius and Swanson, 1999; VERIS 4.x software): this information is displayed in Fig. 5 (bottom panel) in the form of a delay field (Hood *et al.*, 1998a). In the regions of good sensitivity, patient RP1 shows implicit times that are either normal (i.e. the mERG is delayed by 0 ms) or slightly faster than normal (e.g. −2 or −3 ms). The small responses in regions of poor sensitivity are delayed in this patient by 3–7 ms.

Although, in most cases, regions of poor sensi-

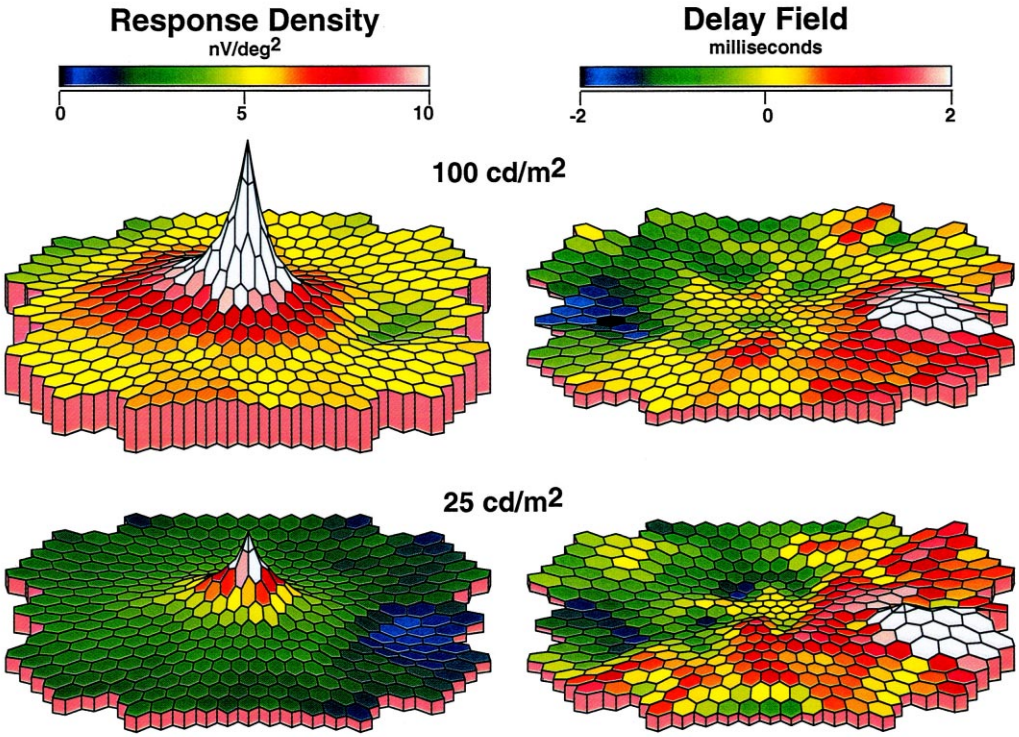

Fig. 13. Three-dimensional plots showing the amplitude (response density in nV/deg^2) and timing (relative delay in ms) variation across the arrays in Fig. 12. These plots were made with VERIS 4.1 software from EDI (San Mateo, CA).

tivity are associated with small, delayed mERGs, amplitude is not always well-correlated with sensitivity loss in patients with RP. There are some patients with reasonably large mERG responses in regions of poor field sensitivity (Hood *et al.*, 1998a). In such cases, these responses are always very delayed, often by more than 10 ms. The mERGs from such a patient, RP5, are shown in

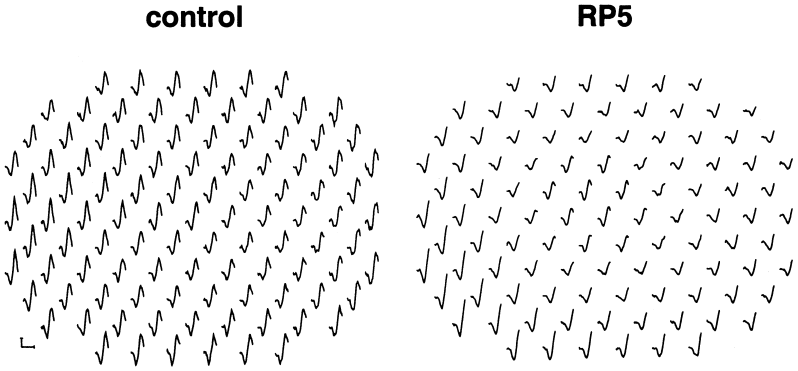

Fig. 14. The mERG responses (A) from a control subject, whose records are in Fig. 12 (upper panel), and from a patient RP5 (B), whose records are in Fig. 15(A), are shown on a time axis from 0 to 35 ms. The horizontal calibration bar indicates 35 ms and the vertical bar 100 nV.

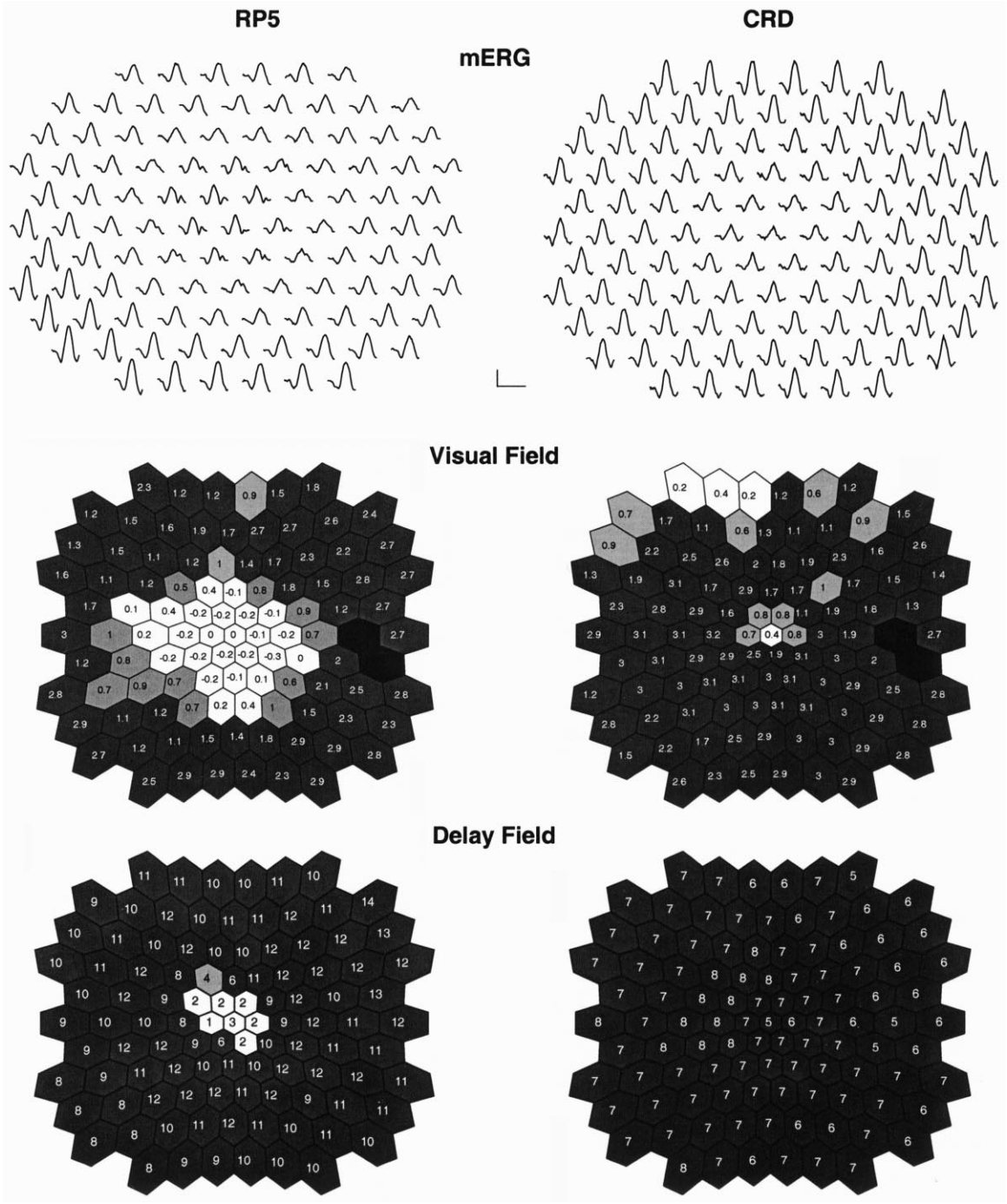

Fig. 15. The mERG records for two patients (top panel). The calibration bars indicate 200 nV and 60 ms. Patient RP5 is the same person as P5 in Hood *et al*. (1998a) but these recordings were made over 3 years later. The records for patient CRD were obtained by Dr. Karen Holopigian at NYU Medical Center and are presented here with her permission and that of Dr. Ron Carr, the patient's ophthalmologist. The visual fields (middle panels) for these patients, obtained by modifying the Humphrey program, show poor correspondence to the mERG responses. The delays in the implicit time (lower panels), on the other hand, show a better correspondence to the visual fields.

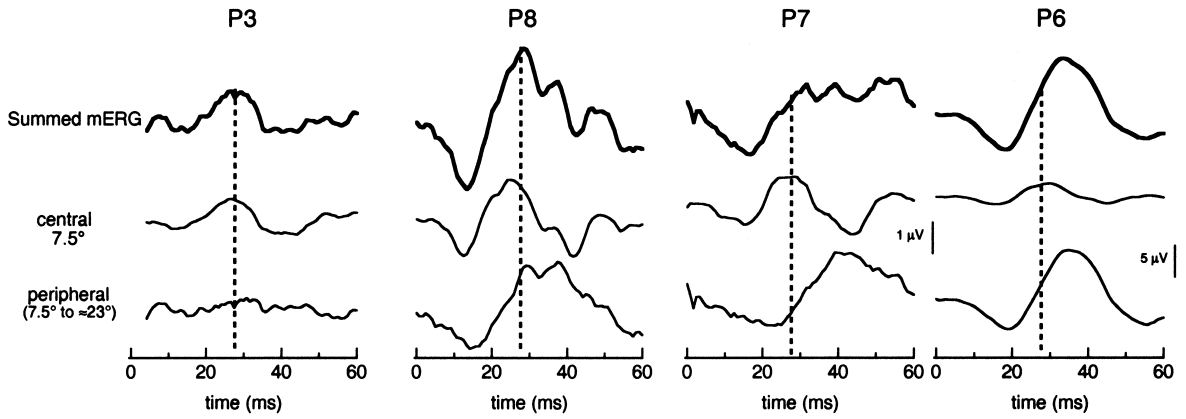

Fig. 16. Each panel contains the summed mERG for all 103 responses (top row), for the central 19 responses in the central 7.5° (second row), or for the remaining 84 responses (bottom row). The calibration bar for P3, P8, and P7 is the same. The vertical dashed lines indicate the time to peak (27.7 ms) of P1 for the peripheral responses of a control group. Modified from Hood *et al.* (1998a) and is reproduced here with permission.

Fig. 15. The mERGs from regions of poor field sensitivity (see middle panel) are relatively large but very delayed (see bottom panel).

3.1.1.1. *Implicit times predict retinal condition*

The timing of mERG responses should prove useful for following both the natural course of RP, as well as the effects of interventions. Reponses from regions of depressed field sensitivity have delayed mERG responses and responses with normal timing indicate regions of normal field sensitivity. However, a value of the visual field within normal limits does not guarantee that the associated mERG response will have a normal implicit time. In fact, delays are observed around the edges of regions of the field within the normal range (see Figs. 5 and 15). Thus, the timing of the mERG appears to be a very sensitive measure of the health of the outer retina.

3.1.2. *Relation to full-field ERG*

It has been accepted for over 30 years that the full-field cone ERG is delayed in patients with RP and that these delays occur relatively early in the disease process (Berson *et al.*, 1969a,b; see Berson, 1993 for a review). A point-by-point comparison of the visual field sensitivities and the mERG responses from patients with RP has helped us to understand this phenomenon (Hood *et al.*, 1998a). The local ERG response is delayed in all cases where the field sensitivity is depressed. It appears then that as soon as an area of the outer retina loses sensitivity, its responses are delayed. In the majority of cases, the delays are associated with small responses as in Fig. 5. But in other cases, the delayed responses can be quite large, as in the case of RP5 (Fig. 15). Presumably these are the relatively unusual patients who have large and delayed full-field ERGs but fields that are small relative to the ERG amplitude.

In any case, the full-field ERG from patients with RP exhibits a range of waveforms and timing. The mERG provides an explanation for this range of responses. Figure 16 shows the summed mERG response of four patients with RP. The top row is the sum of all 103 responses; the middle row is the sum of the central 19 responses; and the bottom row is the sum of the remaining 84 responses. For each patient, the waveform and timing of the central responses are similar to those for control subjects. (All four of the patients in Fig. 16 have good central visual sensitivity and acuity.) In all cases, the responses from the periphery, if detectable, are delayed. However, the waveform and timing of the overall summed mERG (top trace) differ among the

patients. The summed mERG of P3 is dominated by the central responses and thus resembles the central response, while the summed mERG of P6 is dominated by the peripheral responses and resembles the peripheral response. On the other hand, the summed mERGs of P8 and P7 have strange waveforms because these waveforms are a mix of central and peripheral responses. Thus, the summed mERG, and presumably the full-field ERG, of patients with RP will differ and these differences depend upon the relative amount of normal (central) and abnormal (peripheral) retina contributing to the response.

3.1.3. *Diseases of the receptors: a combination of receptor and outer plexiform layer damage*

Table 1 presents a preliminary attempt to relate damage in the different retinal layers to changes in the mERG. We hypothesize that damage to the cone photoreceptor outer segment (e.g. loss of functional pigment molecules) will reduce the peak amplitude of the positive potential P1 and result in moderate delays of its implicit time (i.e. < about 6 ms). In general, any damage to the receptor that destroys the cell or markedly reduces its responsiveness will lead to a decrease in the amplitude of the mERG response.

But how do we account for the patients with large responses in regions of very poor field sensitivity? As noted above, these responses are always very delayed. Hood and Birch (1995, 1996b) demonstrated that changes at the outer segment, as measured by the cone a-wave, could not account for the entire delay in the 30 Hz full-field responses from patients with RP. Further, a loss of quantal absorption by the outer segments can be simulated by decreasing the mean luminance. Although, decreasing the mean luminance can delay the implicit time of the mERG by as much as 6 ms, these delays are only present for low mean luminances where the response amplitude is very small compared to the responses from the patients (see Fig. 11 in Hood *et al.*, 1998a). Thus, we hypothesize that very large delays (e.g. > about 7 ms) or relatively large response amplitudes with moderate delays (e.g. > about 4 ms) imply damage beyond the outer segment. Although we can not precisely locate the damage involved, it must be before the site where the positive potential P1 is generated. The leading edge of P1 is dominated by the response of on-bipolar cells (Horiguchi *et al.*, 1998; Frishman *et al.*, 2000a and Fig. 24). Thus, the damage responsible for the responses that are relatively large and markedly delayed is hypothesized to be in the outer plexiform layer, somewhere in the chain of action between the cone inner segment and bipolar post-synaptic membrane.

There are other diseases that affect the receptors and decrease the amplitude of the mERG. In these diseases as well, the regions of depressed sensitivity in some cases show mERG responses with minor changes in timing while in other cases there are large responses with long delays. According to the framework in Table 1, in some of these patients, damage is restricted primarily to the receptor, while in others the damage includes the outer plexiform layer as well. For example, markedly reduced amplitude with relatively small delays in implicit time such as seen in patient RP1 (Fig. 5) have been seen in patients with Stargardt's macular dystrophy (SMD). The records in Fig. 9 are typical of early SMD as studied by Kretschmann *et al.* (1998a,b). The amplitude in the central field is reduced, but implicit time is only marginally delayed (2 or 3 ms). On the other hand, there are other conditions thought to affect primarily the receptors, which sometimes result in relatively large responses with relatively long delays. These can include cone-rod degeneration (CRD; Fig. 15), progressive cone dystrophy (Holopigian *et al.*, 1998) as defined by Ripps *et al.* (1987), and occult macular dystrophy (Odel *et al.*, 1999) as defined by Miyake *et al.* (1996). The records for a patient with CRD in Fig. 15 (second column) have reduced amplitudes in the central region similar to the patient with SMD. But, like patient RP5 (Fig. 15, first column), this patient has relatively large, but delayed mERG responses in other regions of very depressed visual sensitivity. We hypothesize that these conditions, in addition to affecting receptors, cause damage to the outer plexiform layer and it is this latter damage that is the primary cause of behavioral sensitivity loss in

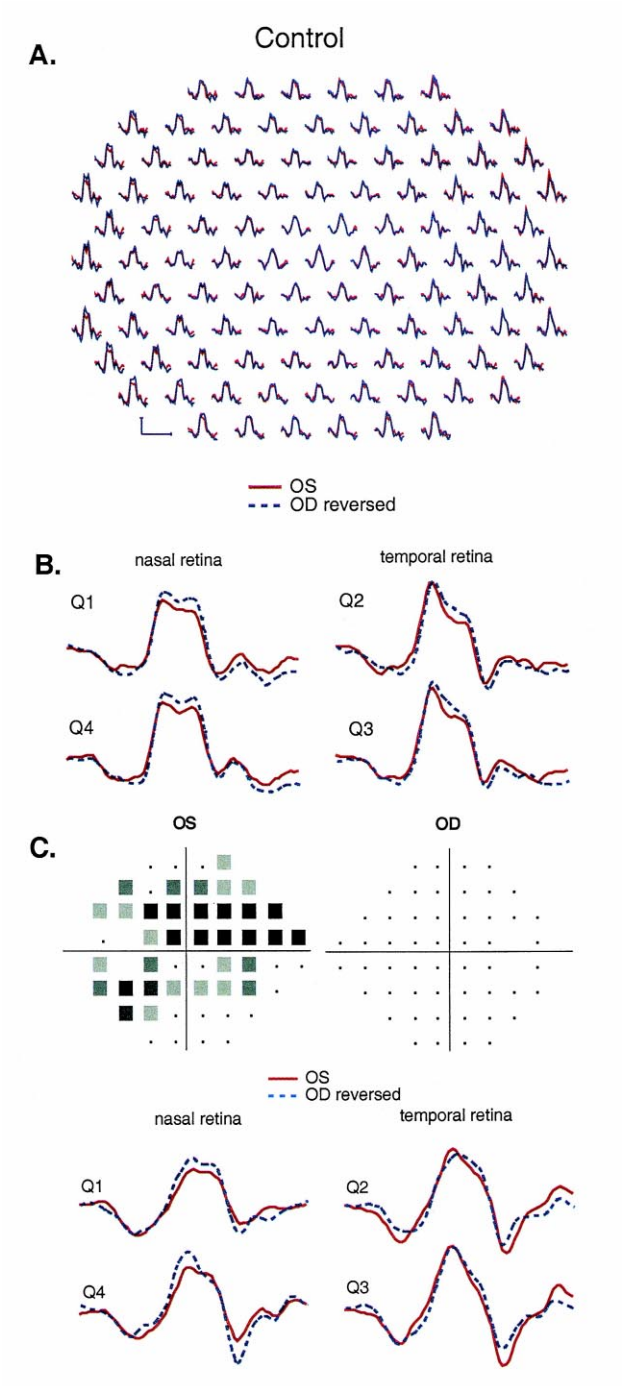

Fig. 17. The mERG responses elicited by an array with a contrast of 50% and a mean luminance of 200 cd/m^2 are shown for both eyes of a control subject; the responses of the right eye horizontally (left–right) reversed so that retinotopic correspondence between the two eyes is preserved (A). These responses were summed across quadrants as shown in Fig. 12(B). The responses from a patient with unilateral glaucomatous defects were summed in the same way, by quadrants (C). Modified from Hood *et al.* (2000b) and is reproduced here with permission.

this subset of patients with relatively large but markedly delayed responses.

3.2. Damage to bipolar cells

3.2.1. *Predicted changes in the mERG*

Most of the mERG is either directly generated by the bipolar cells or is due to inner nuclear layer activity driven by these cells (Horiguchi *et al.*, 1998; Frishman *et al.*, 2000a; see Fig. 24). Thus, damage to these cells will have a profound effect on the mERG and the effect will depend upon the mechanism of the damage. A widespread loss of bipolar cells, for example, should essentially eliminate the mERG; a local or spotty loss should decrease the amplitude of the mERG with little or moderate change in implicit time. A selective loss of on- or off-bipolars will differentially affect the timing of the mERG (see Table 1).

3.2.2. *Diseases affecting the bipolar cells*

Diseases that primarily affect the bipolars are less common than diseases of the receptors. Mizener *et al.* (1997) reported mERGs from two patients with non-cancer associated auto-immune retinopathy whose serum antibodies reacted with the bipolar cell layer of fresh cadaver retinas. Interestingly, consistent with Table 1, their mERGs showed amplitude losses in the areas of visual field defects, with nearly no change in implicit time (Dr. Randy Kardon, personal communication). Possible tests of the effects of altered on-bipolar cell activity should come from the study of patients with complete CSNB (congenital stationary night blindness) and melanoma-associated auto-immune retinopathy. If the defect acts to effectively block the on-bipolar, then Table 1 predicts that the peak P1 should be reduced in amplitude and delayed in time with relatively little effect on the initial negative response (N1). Preliminary reports indicate that the mERG responses from patients with complete CSNB have depressed and delayed P1 responses as suggested by Table 1 (Drs. Kondo and Miyake, personal communication), but an assessment of the degree of agreement must await further study.

3.3. Damage to the inner retina

A number of studies, most in abstract form (see ARVO abstracts 1997–1999), have looked for signs of glaucomatous damage in mERG responses. Some studies have reported changes in mERG amplitude (Chan and Brown, 1999), implicit time (Hasegawa *et al.*, 2000; Fortune *et al.*, 2000) or waveform (Bearse *et al.*, 1996; Hood *et al.*, 1999a, 2000b; Hasegawa *et al.*, 2000). Other studies have failed to find any changes (Vaegan and Buckland, 1996; Vaegan and Sanderson, 1997). The most sophisticated position is that of Sutter and Bearse (1995, 1999) and Bearse *et al.* (1997) who present evidence for a response generated at the optic nerve head and find that glaucomatous damage can reduce this optic nerve head component (ONHC). The Sutter and Bearse theory is considered in Section 4.2.3 in detail but first some basic findings that are emerging from these mERG studies are reviewed.

3.3.1. *The mERG and glaucoma: changes are not reliable and not necessarily local*

The contrast of the multifocal display has been reduced in an attempt to detect local glaucomatous damage (Bearse and Sutter, 1998; Hood *et al.*, 1999a, 2000b). Bearse and Sutter (1998) suggested that decreasing the contrast of the stimulus might increase the relative contribution from the inner retina. The records in Fig. 17(A) are the mERG responses from a control subject with the contrast lowered to 50%.[2] In the multifocal paradigm, a mean luminance of 100 cd/m^2 and a contrast of 50% describes a display with "light gray" and "dark gray" hexagons, which

[2]Saying that a mERG stimulus has contrast of 50% oversimplifies the potential differences between it as opposed to the 100% contrast stimulus. In theory the response to the 100% stimulus will be the difference between the response to the local flash and the "response" to darkness (or at least the minimum of the screen). And, the response to the 50% contrast will be the difference between the responses to two local flashes of different intensities.

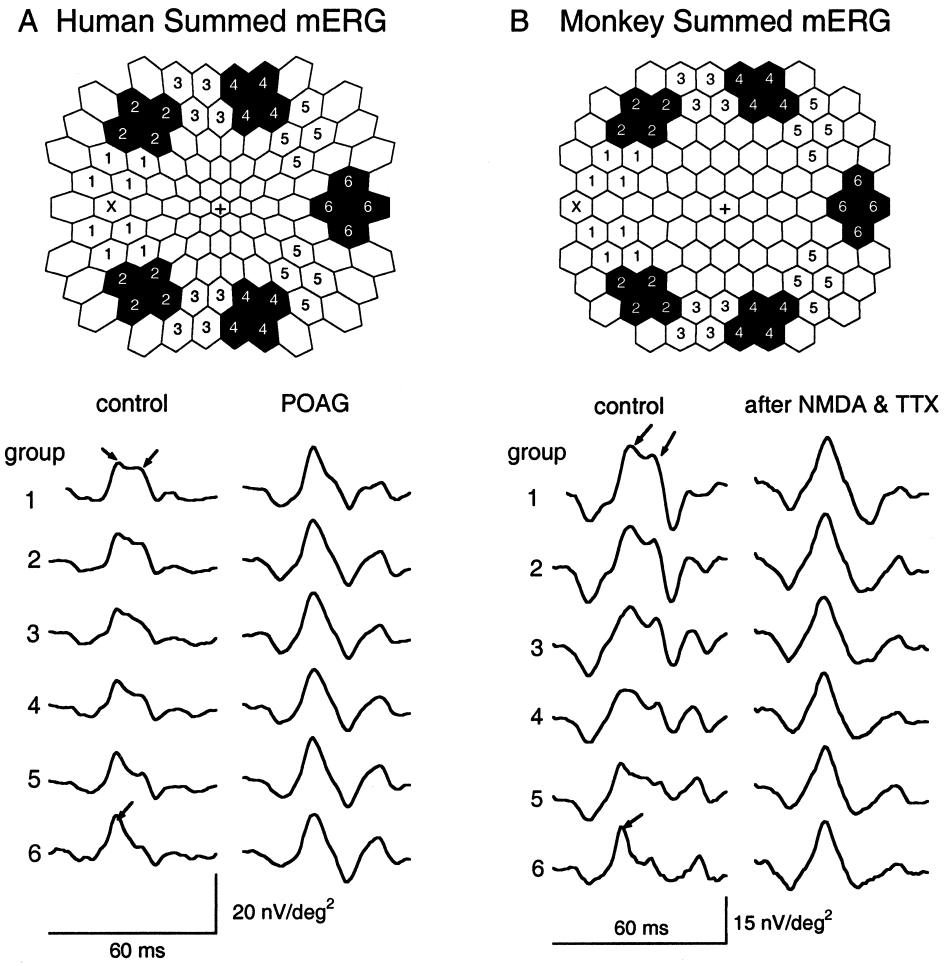

Fig. 18. The mERG responses from a control subject and a patient with glaucoma are shown summed for regions that are equidistant from the center of the fovea, "+", but different distances from the blind spot, "X" (A). A similar analysis is shown for responses from a control monkey and the same eye treated with NMDA and TTX (B). Modified from figures in Hood *et al.* (1999a) and reproduced here with permission.

are set to 150 and 50 cd/m^2, respectively. With a 50% contrast display, the mERG responses show noticeable naso-temporal variations in waveform (Hood *et al.*, 1999a, 2000b). This is an important observation as naso-temporal variations in waveform have been hypothesized to be due to ganglion cell activity (see Sutter and Bearse, 1999 and Section 4.2.3). The naso-temporal variation in Fig. 17 is similar in the two eyes of a control subject. In Fig. 17(A), the mERG records from both eyes of a control subject are shown, with the responses for the right eye reversed so that responses from corresponding regions of the retina are presented together. The naso-temporal variation can be seen in the responses summed over quadrants (Fig. 17(B)), but is more salient in Fig. 18, where the summed mERG responses are shown for small regions that are equidistant from the fovea but fall at different distances from the optic disk. Compared to the temporal retina (e.g. groups 5 and 6), the responses from the nasal retina (e.g. groups 1 and 2) appear to be broader with a more prominent second peak (see arrows).

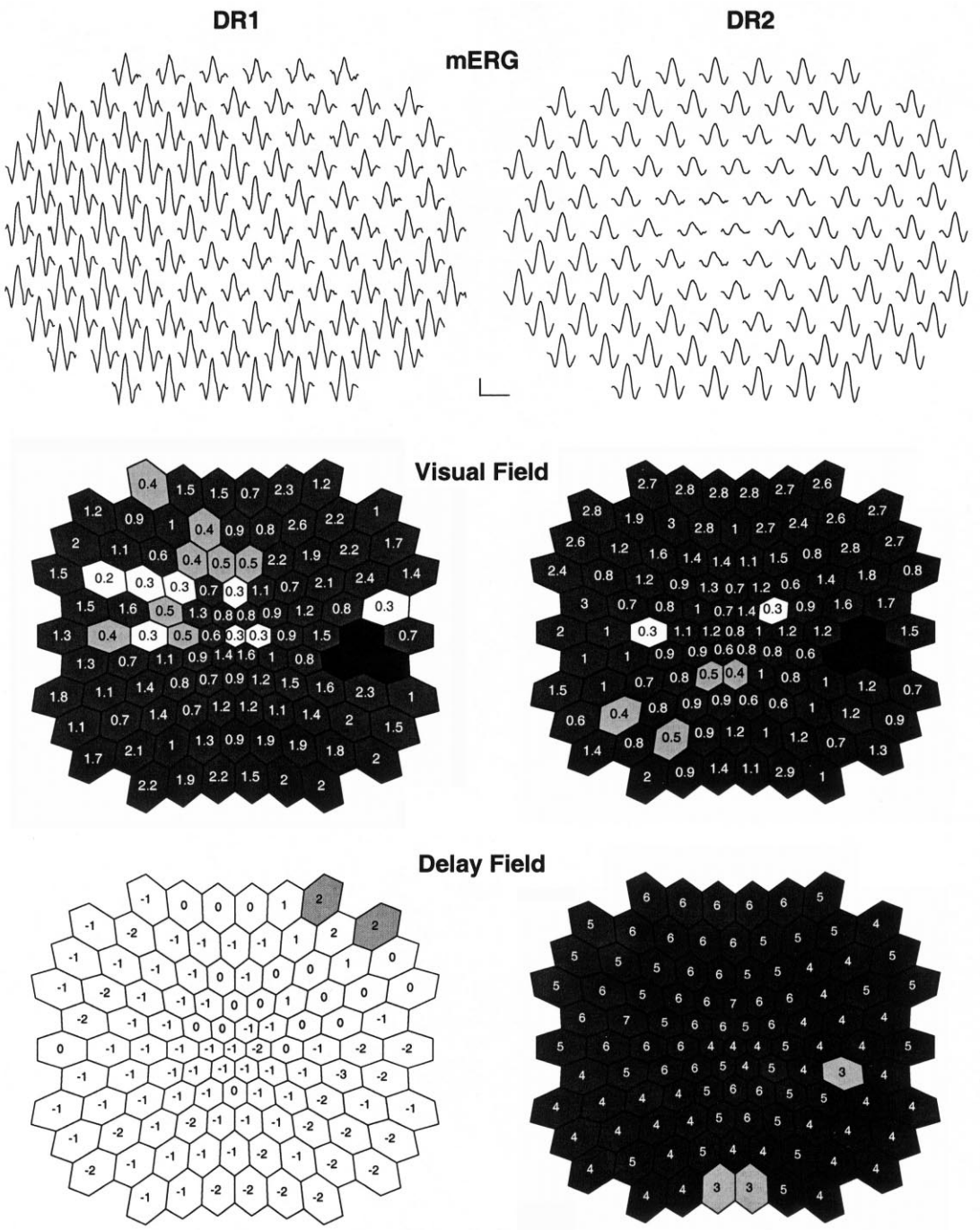

Fig. 19. The mERG records for two patients (top panel) with diabetic retinopathy (level 3) and clinically significant macular edema. The calibration bars indicate 130 nV and 60 ms. Patient DR1 and DR2 correspond to patients P10 and P9 in Greenstein *et al.* (2000). The visual fields (middle panels) for these patients, obtained by modifying the Humphrey program, show poor correspondence to the mERG responses. The delays in the implicit time (lower panels) show a better correspondence to the visual fields for DR2, but not DR1. Modified from figures in Greenstein *et al.* (2000) and reproduced here with permission.

Some, but by no means all, patients with glaucoma have substantially reduced naso-temporal variation in mERG waveform. The mERG responses from a patient with open angle glaucoma (POAG) in Fig. 18(A) (bottom) are far more similar across the retina than are the control records (Hood *et al.*, 1999a). This decreased naso-temporal variation can be seen in other patients with glaucoma. In fact, it is possible to see differences in the mERG from the two eyes of patients with glaucoma with the more affected eye showing less naso-temporal variation (Hasegawa *et al.*, 2000; Hood *et al.*, 2000b).

However, problems exist for any simple linking of glaucomatous damage to mERG changes. First, the changes in the mERG do not correlate well with local field changes (Fortune *et al.*, 2000; Hood *et al.*, 2000b). Second, although the naso-temporal variations observed in patients with glaucoma are probably produced by variations in the contribution from action potentials (discussed below), ganglion cell damage per se is not a sufficient condition to eliminate it. Some patients with substantial field loss show normal-appearing mERG responses with normal naso-temporal variations. The records in Fig. 17(C) illustrate this point. The records from both eyes are similar to those from the control and to each other, in spite of the fact that the left eye has an extreme field loss while the right eye has an essentially normal visual field. Similarly, patients with ischemic optic neuropathy (ION), in which substantial ganglion cell degeneration must surely have occurred, can also have normal appearing mERG responses with normal naso-temporal variations (Hood *et al.*, 2000b). Therefore, most of the changes seen in the mERG responses from patients with glaucomatous damage do not appear to be directly due to ganglion cell damage per se.

In any case, it remains to be seen if the mERG will be the long sought-after technique for identifying early damage in glaucoma. Sutter and Bearse have designed a "global flash paradigm" that may provide a better mERG method (Sutter and Bearse, 1998; Sutter *et al.*, 1999). However, others have suggested that the multifocal VEP (Baseler *et al.*, 1994) is a more promising candidate (Klistorner *et al.*, 1998; Hood and Zhang, 2000; Graham *et al.*, 2000; Hood *et al.*, 2000c).

3.3.2. *Diabetes: more than one level of damage*

A few recent studies have recorded mERGs from patients with diabetes. In some patients, changes can be readily detected while in others the mERG appears normal (cf. Palmowski *et al.*, 1997; Fortune *et al.*, 1999; Greenstein *et al.*, 2000). Further, these changes seem to correlate with local damage, as seen on fundus photographs (Fortune *et al.*, 1999) or visual fields (Greenstein *et al.*, 2000), in some patients but not in others. Consider the data from two patients with diabetic retinopathy in Fig. 19 (Greenstein *et al.*, 2000). Both patients have level three retinopathy with CSME (clinically significant macular edema) and both show extensive losses in visual field sensitivity. Further, the central mERG responses are reduced in amplitude secondary to the CSME. However, in one case, DR1, the peripheral responses have normal timing (Fig. 19, bottom panels) while in the other, DR2, the responses are markedly delayed. My hypothesis, based upon the framework in Table 1, is that the site of retinal damage responsible for the field loss is different in the two patients: in one case, DR1, the damage is probably in the inner retina, while in the other, DR2, it is in the outer retina.

3.3.3. *Summary and conceptual framework*

Table 1 shows my tentative conclusions about damage to the inner retina. The accumulated evidence suggests that the inner retina contributes to the mERG, but that damage to the ganglion cell is not a sufficient condition to eliminate this contribution. However, questions remain. What is the source of the inner retinal contribution affected in some patients with glaucoma? And, what is the relationship between this inner retinal contribution and the ONHC proposed by Sutter and Bearse? We return to these questions below when we examine the results from monkeys in

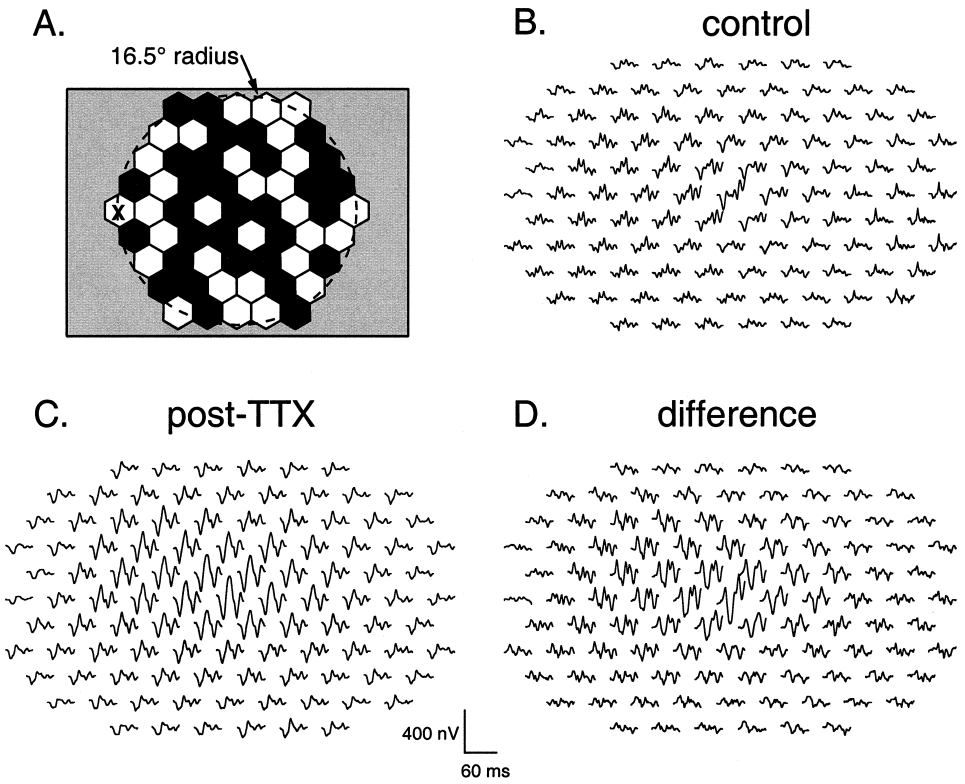

Fig. 20. The mERG is recorded from anesthetized monkeys to an array of 103 equal-size hexagons (A). The mERG responses are shown for the control condition (B) and after an intravitreal injection of TTX. TTX removes a large component from the mERG (D). Reproduced by permission from Hood *et al.* (1999c).

which inner retinal activity has been chemically blocked.

4. CELLULAR CONTRIBUTIONS TO THE MONKEY MERG

4.1. Recording the mERG from monkeys

Recently, mERGs have been recorded from monkeys (Hare *et al.*, 1999; Hood *et al.*, 1999a,b,c; Frishman *et al.*, 2000a,b). In these experiments, the monkey viewed a display with hexagons of equal size (Fig. 20(A)). The records in Fig. 20 are from the left eye of a monkey and the "x" in panel A indicates the approximate location of the optic nerve head (see Hood *et al.*, 1999a,c for details). The mERG responses for the control condition show large naso-temporal variations in waveform. These variations are easy to see in Fig. 21 where the control records are grouped from different regions at different distances from the optic nerve head. Although the naso-temporal variations are qualitatively similar to those from human controls (see Fig. 18(A)), they are more dramatic in the case of the monkey. This appears to be due to a larger inner retinal contribution in the case of the monkey mERG (Hood *et al.*, 1999a, 2000b).

4.2. Inner retinal contributions

4.2.1. *The role of action potentials*

Action potentials from ganglion cells can be blocked by tetrodotoxin (TTX), which blocks voltage-gated sodium channels. In addition to ganglion cells, some amacrine cells (Stafford and

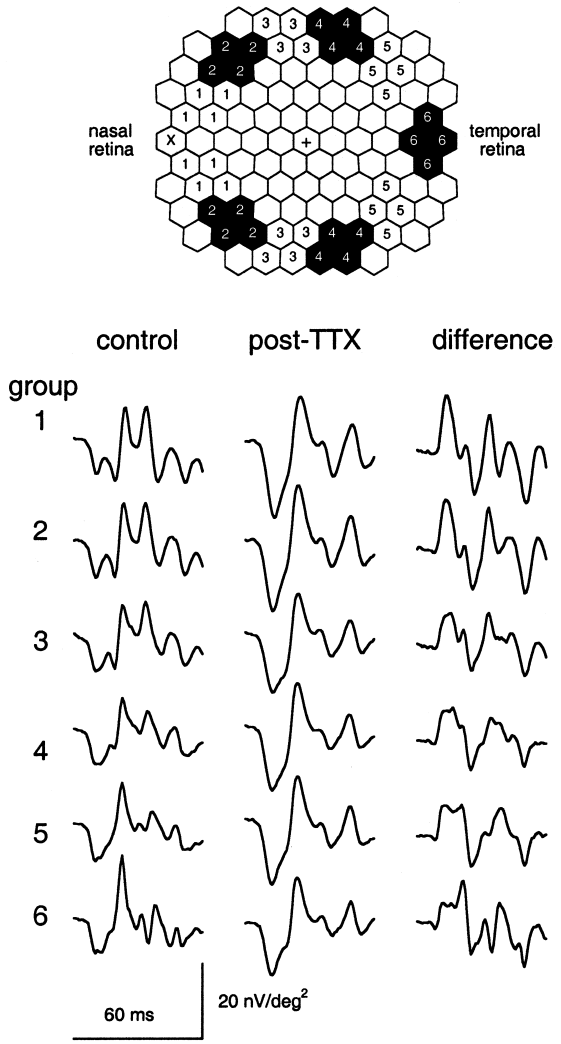

Fig. 21. The mERG responses from Fig. 19 are shown summed for regions that are equidistant from the center of the fovea ("+") but at different distances from the blind spot ("X"). Reproduced by permission from Hood *et al.* (1999c).

Dacey, 1997) and perhaps the interplexiform cells fire sodium-based action potentials. Viswanathan *et al.* (1999) identified a TTX-sensitive response in the monkey's (macaque) full-field ERG and showed it to be diminished in experimental glaucoma. This is consistent with other work from this group demonstrating altered ERG waveforms in experimental glaucoma (Frishman *et al.*, 1996; Viswanathan *et al.*, 2000). There is also a large TTX-sensitive contribution to the mERG. This can be seen in Fig. 20(D), which shows the difference between the records before (panel B) and after (panel C) administration of TTX. TTX essentially eliminates the naso-temporal variations (see Fig. 21). Before TTX, there is a large naso-temporal difference in waveform; after TTX this variation is no longer present. Thus, the naso-temporal variations in the waveform of the mERG depend upon cells that fire action potentials.

4.2.2. *Relevance to human diseases of the ganglion cell*

In light of the results from the TTX-treated monkeys, how do we understand the naso-temporal variations in the human mERG and the fact that they are absent in some, but not all patients with ganglion cell damage? One possibility is that the naso-temporal variations are not due to ganglion cell activity per se in either the monkey or human. For example, the variations may depend upon the amacrine and/or interplexiform cells that carry action potentials, or on the connections made by ganglion cells to these cells. The implication is that those patients who show modified naso-temporal variations in waveform have damage that extends into the inner retina, beyond the ganglion cell body and axon. A second possibility is that the naso-temporal variation depends upon the integrity of the glial cells or myelin sheaths near the optic disc and that action potentials generated by ganglion cells are necessary, but not sufficient, to produce the TTX-sensitive contribution to the monkey mERG. According to this second explanation, glaucoma must damage either the structures in the optic nerve head, or a sufficiently large number of ganglion cells, for the mERG to be altered. This could explain why we observe changes in some patients but not in others and why these changes do not appear to be localized. Of course, it is entirely possible that the damage necessary to change the mERG includes both the connections to cells distal to the ganglion cell as well as glial cells near the optic disc, in addition to the ganglion cells themselves.

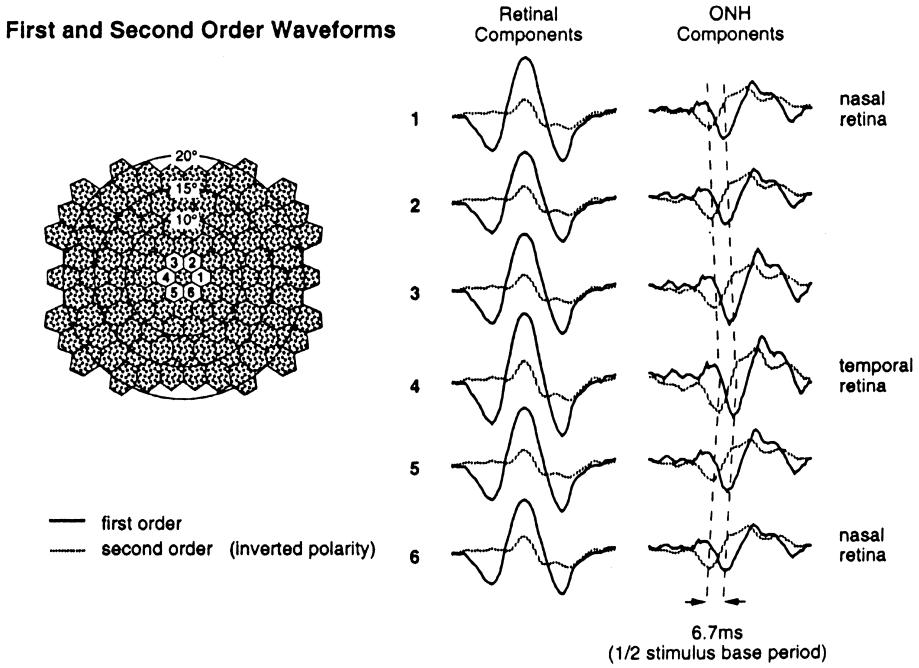

Fig. 22. The retinal and optic nerve head (ONH) components are shown for the mERG responses around the first ring. Reproduced by permission from Sutter and Bearse (1999).

4.2.3. *The optic nerve head component (ONHC) theory*

Sutter and Bearse (1999) hypothesized that the mERG has two components, a retinal component and an ONHC. The mERG is assumed to be the sum of these two components. The retinal component has the same shape for any given distance from the fovea. The ONHC also has the same

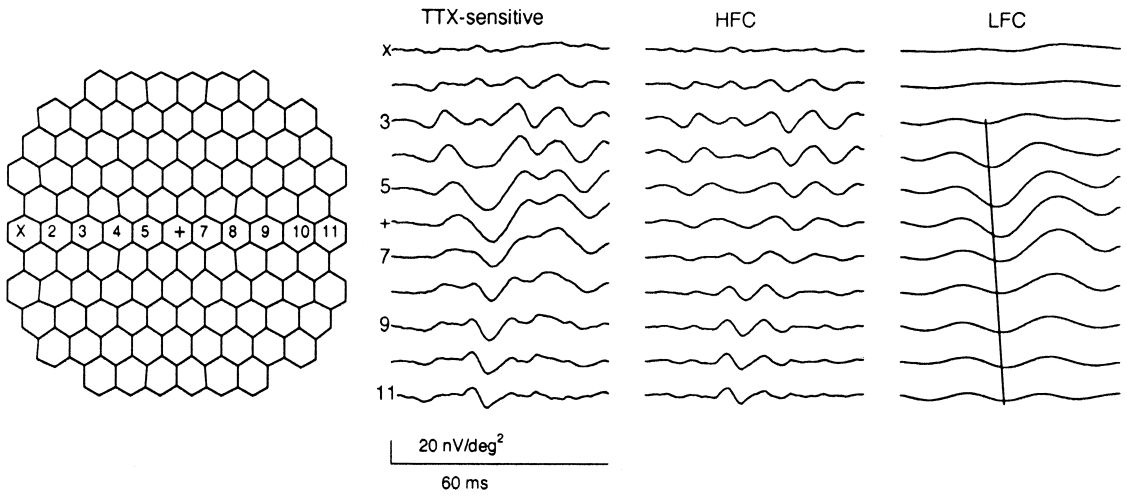

Fig. 23. The TTX-sensitive contribution to the mERG responses is shown for the hexagons across the horizontal midline. These responses are divided into a high frequency (HFC; >75 Hz) and low frequency (LFC; <75 Hz) components. Reproduced by permission from Hood *et al.* (1999b).

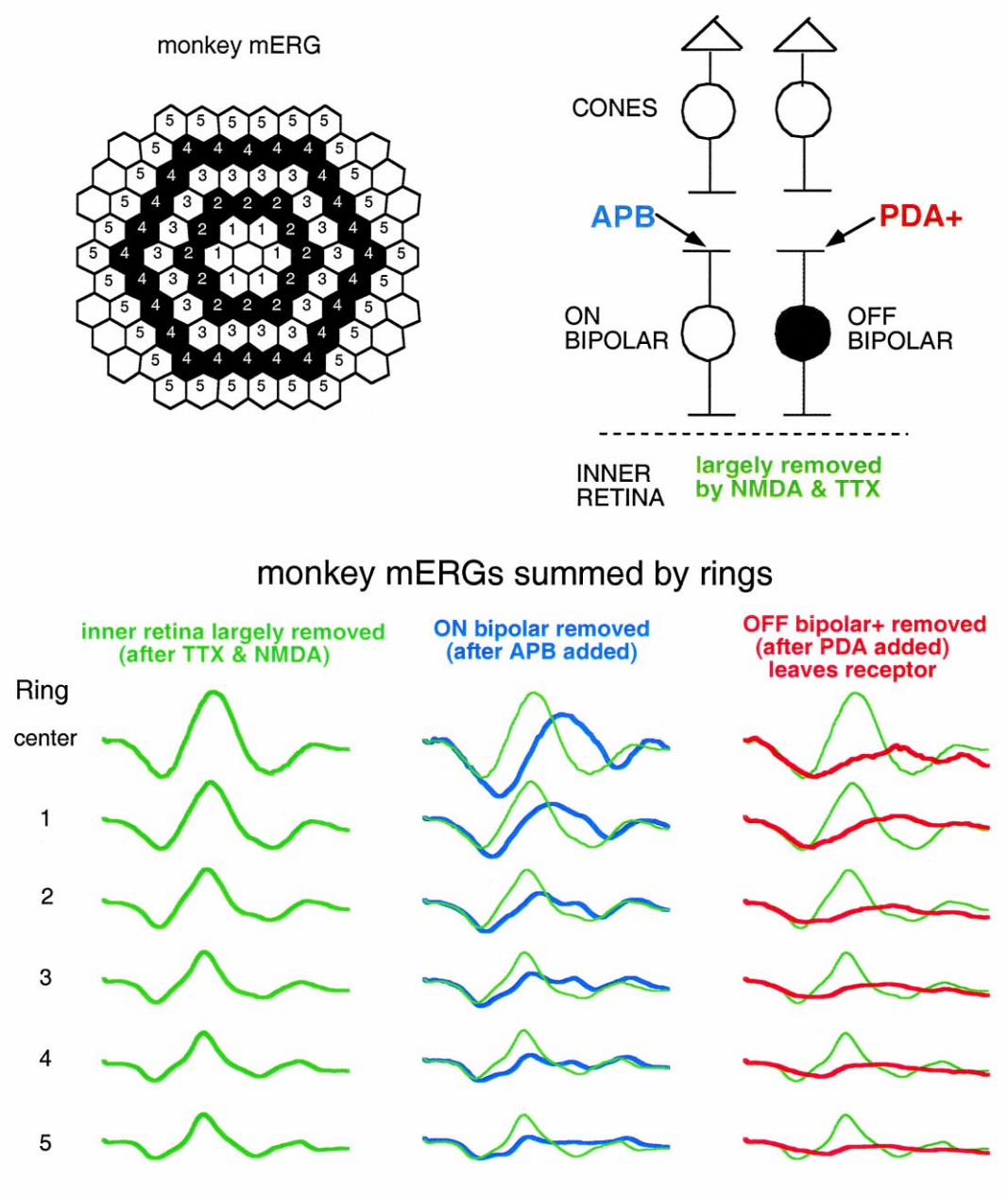

Fig. 24. A monkey's mERG responses, summed by rings as in Fig. 10, are shown after serial, intravitreal injections of TTX and NMDA, APB, and PDA. Reproduced by permission from Frishman et al. (2000a).

overall shape for any given distance from the fovea, but is displaced in time depending upon the distance from the ONH. Sutter and Bearse developed an algorithm to extract the ONHC and examples of these responses can be found in Fig. 22 for mERG responses to a typical high contrast display. Although a large-scale study has yet to be reported using this algorithm, there is some evidence suggesting that glaucomatous damage can eliminate the ONHC (Bearse *et al.*,

1996). In its strong form, the theory attributes all variation in mERG waveform, except the variation in implicit time with distance from the fovea, to the ONHC. I will call this strong form "the ONHC theory". In particular, the ONHC theory predicts that the naso-temporal variations in waveform must be due to the ONHC. Below the ONHC theory is viewed in light of the monkey and patient data.

4.2.3.1. *The monkey mERG and the ONHC*

The fact that TTX removes all naso-temporal variation is consistent with the ONHC theory. In addition, the mERG responses are modified in monkeys by experimentally-induced glaucoma (Hare *et al*., 1999; Frishman *et al*., 2000b) and these changes bear some resemblance to the effects of TTX (Frishman *et al*., 2000b). However, the TTX-sensitive contribution does not look like an ONHC. Figure 21 (rightmost column) shows the contribution removed by TTX at different distances from the ONH. This contribution does not behave as predicted by the ONHC theory; the ONHC should be of the same shape, but shifted in time with distance from the ONH. On the other hand, Hood *et al*. (1999b) found that the low frequency component (LFC) of this contribution, obtained by removing the frequencies above 75 Hz, does behave as predicted by ONHC theory. The TTX-sensitive contribution is shown in Fig. 23 for responses to the hexagons across the horizontal midline. The LFC has the same waveform across the retina; it is slower in the fovea and temporal retina compared to the nasal retina (see line in right-hand column of Fig. 23); its amplitude varies with distance from the fovea; and it qualitatively resembles Sutter and Bearse's ONHC (compare rightmost columns in Figs. 22 and 23). The high-frequency component (HFC) in Fig. 23, on the other hand, appears to have two distinct waveforms in the nasal retina versus the temporal retina.

At this stage, the monkey mERG results do not provide a definitive test of the ONHC theory. The naso-temporal variations seen in the HFC in Fig. 23 may be inherent to the inner retina and represent a violation of the ONHC theory for the monkey mERG. On the other hand, the HFC may itself be a combination of a retinal component and an ONHC (E. E. Sutter, personal communication). Future analysis should resolve this issue.

4.2.3.2. *The human mERG*

According to the ONHC theory, the naso-temporal variation in the human mERG should be due to the ONHC. Thus, ganglion cell damage should reliably decrease this variation. We saw above that it does not. Thus, it is likely that there are inner retinal contributions contributing to the naso-temporal variations in the human mERG that are not coming from the ONH. How much of the human mERG is due to the ONHC, and how much is due to other inner retinal contributions, remains to be determined.

4.2.4. *Other contributions from the inner retina*

TTX does not remove the entire contribution from the inner retina in the monkey mERG. Adding NMDA after TTX changes the waveform of the mERG (Hood *et al*., 1999a). NMDA depolarizes ganglion cells and at least some types of amacrine cells (see Massey and Maguire, 1995 for review). After NMDA and TTX (Fig. 18B, lower right column of responses), the monkey's mERG responses more closely resemble those of the patient with glaucoma in Fig. 18 than do those after TTX only (Fig. 21). The similarity here is consistent with the suggestion that glaucomatous damage can be distal to the ganglion cell axon (Hood *et al*., 2000b).

4.3. Outer retinal contributions

4.3.1. *Receptor and bipolar contributions to the monkey mERG*

The contributions of the cone receptors and the bipolars can be estimated by chemically blocking the activity of specific cell types (Fig. 24; Frishman *et al*., 2000a). The combination of TTX and NMDA should block most of the inner retinal (i.e. amacrine and ganglion cell) contri-

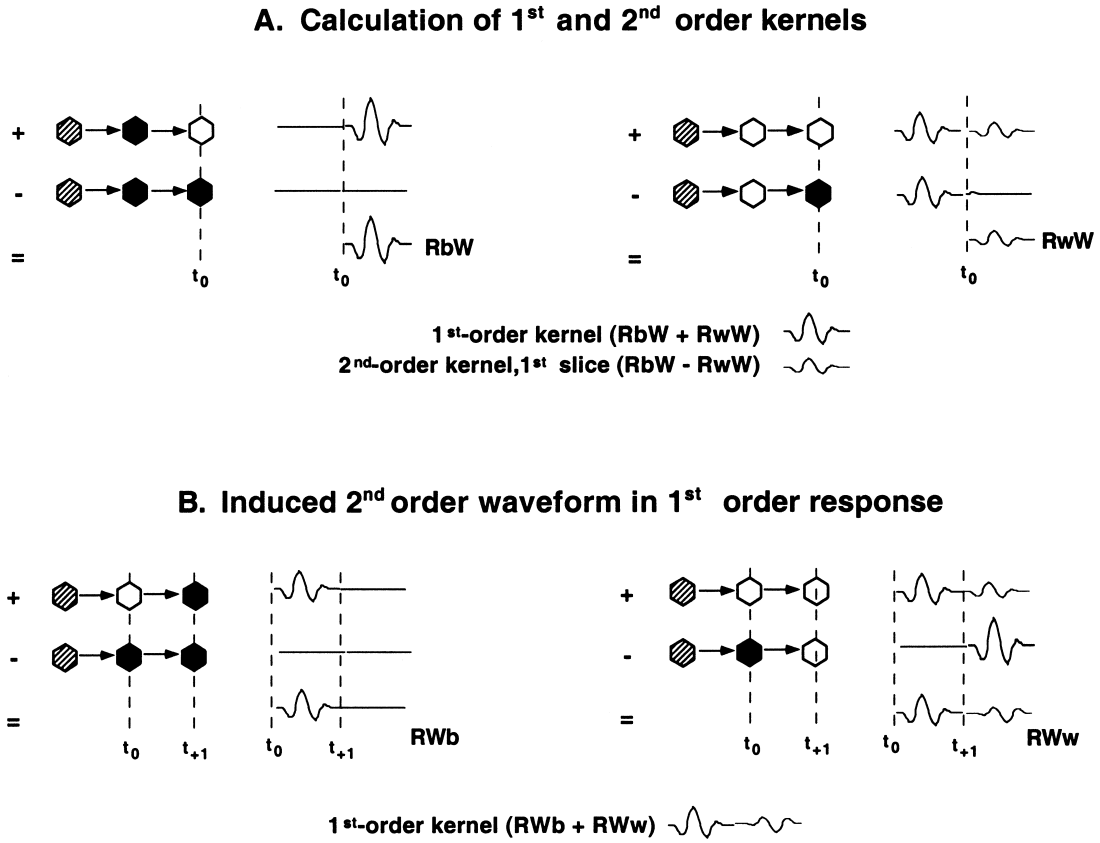

Fig. 25. The sequences in Fig. 2 are rearranged to illustrate how the first- and second-order kernels are related (A) and why there is an induced second-order waveform in the first-order kernel (B). As in Fig. 2, open hexagons indicate a flash occurred on that frame change; the black hexagons indicate a flash did not occur; and the hexagons with the diagonal lines indicate a frame that could have had either a flash or no flash.

butions to the mERG. The mERG responses remaining are shaped by both on- and off-bipolar activity as has been shown in the case of the primate, cone-mediated, full-field ERG by Sieving *et al.* (1994). APB blocks synaptic input to these cells. Removing the contributions of the on-bipolars with APB delays the positive peak P1 of the monkey's mERG (Fig. 24, middle column). The activity of the on-bipolar cells appears to dominate the leading edge and peak of P1: without the on-bipolar contribution, P1 is delayed and smaller. Frishman *et al.* (2000a) obtained an estimate of the receptor contribution to the mERG by adding PDA after APB. PDA blocks transmission to the remaining cells that the photoreceptors contact in the outer plexiform layer: the off-bipolar and horizontal cells. It is clear in Fig. 24 that the cone receptors are making a considerable contribution to the central, but not the peripheral responses. Outside the central three rings (about 13°), the leading edge of N1 is nearly entirely shaped by the off-bipolar response. Thus, the cone receptor contribution to the a-wave of the full-field ERG for a similar, moderate intensity will be minimal (Bush and Sieving, 1994; Sieving *et al.*, 1994). However, it appears that the initial negative potential of the central responses of the mERG has a large receptor contribution, at least in the monkey.

4.3.2. *Implications for diseases of the human retina*

Given the large inner retinal contribution to

the monkey mERG, care must be exercised in extrapolating to the human mERG. However, the consequences of blocking bipolar input to the monkey mERG (Fig. 24) provide a guide to what bipolar damage will do to the waveform of the human mERG. First, the large delayed P1 seen in some patients with outer retinal diseases is very likely due to a large delay in bipolar cell responses, especially the on-bipolars, which dominate the leading edge. We cannot say where, in the chain of activity from cone inner segment to the depolarizing of the on-bipolar, the cause of the delay is located, but we can conclude that the on-bipolar response is delayed in these patients. Second, diseases that remove the on-bipolar contribution (e.g. CSNB) should affect the leading edge of P1, delaying its onset and substantially reducing its peak. Loss of off-bipolars should decrease the amplitude of N1 (and perhaps even increase the peak amplitude of P1). Losing both bipolar inputs should essentially eliminate the mERG, leaving a barely detectable negative-going response.

5. THE SECOND-ORDER KERNEL AND RELATED TOPICS

To understand and to make effective use of the mERG technique, one should have at least a rudimentary knowledge of second order responses. This section provides an introduction to the second-order kernel and attempts to illustrate why a basic understanding of this material is important. Although this section is meant as a tutorial, many readers will find this material more difficult than the earlier sections of this review. For these individuals, Section 5 is best tackled after a brief rest. For a more complete description of higher-order kernels, see the excellent tutorial by Sutter (2000).

5.1. What is the first slice of the second-order kernel?

The second-order kernel is a measure of how the mERG response is influenced by the adaptation to successive flashes. The first slice of the second-order kernel measures the effect of an immediately preceding flash, the second slice of the second-order kernel measures the effect of the flash two frames away, and so on. Fig. 2B presents a schematic of how the first slice of the second-order kernel is calculated. The key to understanding this kernel is to compare the two responses indicated by the arrows. The upper bold arrow in Fig. 2B indicates the response to a flash preceded by a flash; the lower bold arrow indicates the response to a flash preceded by no flash (a dark hexagon). If these two responses are not identical then there is a second-order (first slice) kernel, and it is calculated by subtracting one response from the other. In particular, as indicated in Fig. 2B, the second-order kernel is obtained by adding all the records following a change from either white-to-black or black-to-white and subtracting all the records following no change. In this schematic, the preceding flash is assumed to scale down the response by a multiplicative factor.

Fig. 25 illustrates why the first slice of the second-order kernel is, as implied above, the difference between two components that make up the first-order kernel. In Fig. 25(A), the four frame sequences in Fig. 2(B) are rearranged. The difference between the responses to the two sequences on the left produces an estimate, RbW, of the first-order kernel for those frames that were preceded by a black hexagon. The difference between the responses to the two sequences on the right produces an estimate, RwW, of the first-order kernel for those frames that were preceded by a flash. [Read RwW as the response to a flash, W, preceded by a flash, w; and RbW as the response to a flash, W, preceded by a black hexagon, b]. Mathematically, adding together RbW and RwW produces the overall first-order kernel, exactly as obtained in Fig. 2A. Subtracting RbW from RwW produces the first slice of the second-order kernel, as in Fig. 2(B). This is not surprising: these are the same four frame sequences as in Fig. 2, just grouped differently.

This alternate grouping, however, leads to an important observation, one that makes clear why the second-order kernel has important implications for the first-order kernel. Fig. 25 shows that the first-order kernel is comprised of two populations of responses with different waveforms. In the example here, the two waveforms

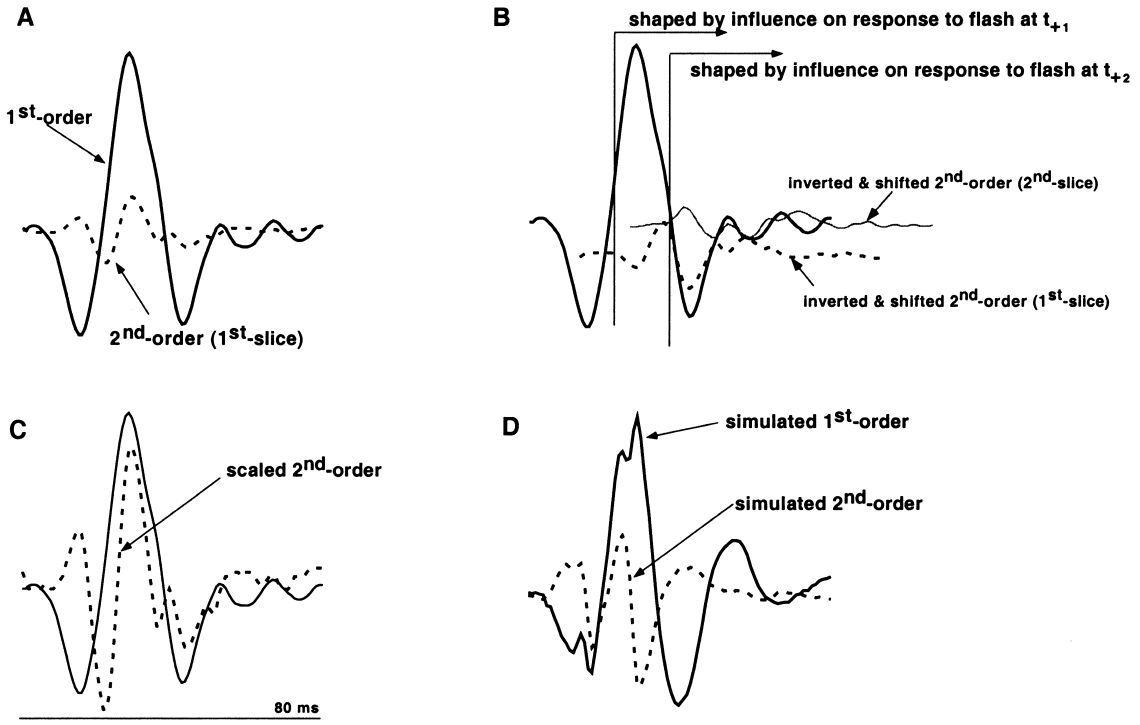

Fig. 26. The waveform of the first-order kernel to the flash at t_0 is shaped by the influence of preceding flashes and by the influence of the flash at t_0 on the response to subsequent flashes. These influences appear in the form of a second-order kernel (dashed and dotted in A and B). The nonlinear mechanism producing the second-order kernel is not a simple (static) gain change (C). The full-field simulation in Fig. 27 produces rough approximations (D) to the mERG waveforms (A). All traces are 80 ms long.

are shown as scaled versions of one another; as a result, the first- and second-order kernels have the same shape. We will see below that this simple picture is probably seldom true, that the shape of the second-order kernel is typically very different from the first-order kernel, and that these differences in waveform (the differences between RwW and RbW) contain important information about the non-linearities in the retina.

5.2. The induced version of the second-order kernel in the first-order kernel

Just as a response to a flash at time t_0 is influenced by a flash at t_{-1}, so will the flash at t_0 influence the response to a flash at t_{+1} and this influence will be seen in the first-order kernel (Sutter and Bearse, 1998; Sutter, 2000). Fig. 25(B) illustrates this point: four frame sequences are shown, as in Fig. 25(A), but here they are arranged so that the four possible flash combinations, along with the associated responses, are shown for frames t_0 and t_{+1}. Again, the same mathematics as in Fig. 25(A) and 2(A) are applied. The first-order kernel is obtained by adding the responses to the sequences in which there is a flash at t_0, and subtracting the responses to the sequences in which there is a black hexagon at t_0. However, we can now visualize a longer portion of the waveform, out to 26.7 ms (the duration of two frames). Starting at t_{+1}, a second response component appears in the waveform. A quick comparison to Fig. 25(A) makes it apparent that this response component is an inverted second-order kernel associated with the flash at t_{+1}, and is thus shifted by 13.3 ms (the temporal separation between frames t_0 and t_{+1}). That is, the waveform of the first-order

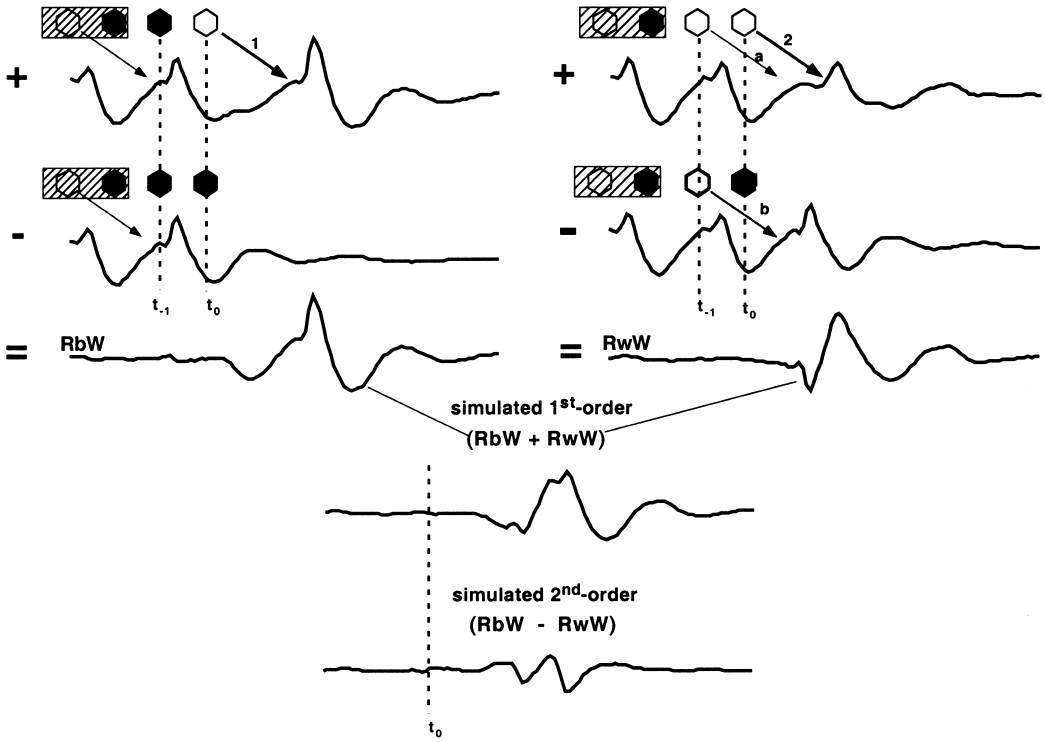

Fig. 27. Full-field ERG responses to a train of brief pulses designed to simulate the multifocal stimulus train. The four possible combinations of two-flash sequences are shown in the same form as in Fig. 25. See text for details.

kernel contains an inverted copy of the second-order kernel. Sutter (2000) calls this an "induced component". In the schematic of Fig. 25(B), the two responses are shown as non-overlapping, readily separable waveforms. In reality, however, the first-order kernel extends well beyond the duration of one frame, and thus overlaps the induced version of the second-order kernel.

5.3. The first-order kernel: more complex than it appears

The summed mERG response (first-order kernel) from the multifocal array in Fig. 6(B) is shown in Fig. 26(A), along with the summed second-order (first slice) kernel for the same records. In Fig. 26(B), this second-order kernel is shown inverted and shifted by 13.3 ms (the second slice of the second-order kernel is also shown, inverted and shifted by 26.7 ms). This follows the insight gained from Fig. 25(B), above. Clearly the waveform of the first-order kernel is affected by the influence that a flash has on the response to the next flash: components equivalent to the second-order slices clearly contribute to the later portion of the first-order waveform. This contribution begins earlier than the peak (P1) of the response, helps to shape P1, and plays a part in creating the second negative component N2. The influence of the flash at t_0 on the response to the flash at t_{+2} (the second slice) and at t_{+3} (the 3rd slice, not shown) also helps to shape the first-order kernel by contributing to the late wavelets.

Since the mERG waveform does not resemble the full-field ERG, we know that the m-sequence is influencing its shape. The fact that a second-order kernel exists indicates that part of this influence is due to the preceding flash. That is, as pointed out above, the first-order kernel is made up of waveforms that differ depending upon the

immediately-preceding flash history. This is illustrated further in the simulations of Fig. 27 below.

5.4. The second-order kernel: of first order importance

The shape of the second order kernel provides important information about the nature of the nonlinear (adaptive) mechanisms of the retina. If the preceding flash acted to scale down the response (a multiplicative gain), then, as schematized in Figs. 2 and 25, the second-order kernel would be a smaller version of the first-order kernel. Fig. 26(C) shows this is not the case. Here, the second-order kernel is scaled to have about the same trough-to-peak amplitude as the first-order kernel. The waveform of the second-order is not as would be predicted, from the first-order kernel, by a simple multiplicative gain change or by response compression, another common nonlinear mechanism (see Fig. 11 in Sutter and Bearse, 1999). The preceding flash is probably adapting different components of the response to different extents and perhaps via different mechanisms.

5.5. Full-field simulation of the first- and second-order kernels

To help us to understand the mechanisms involved, the first- and second-order kernels can be simulated with the full-field ERG (Hood and Seiple, unpublished; see Hood *et al.*, 1998b for a simulation of the rod mERG). Fig. 27 shows the results of a simulation using a train of brief, full-field flashes of about the same intensity as the multifocal flashes used to elicit the responses in Fig. 26. As in Fig. 25, four sequences are shown; the hexagons, in this case, denote full-field flashes, separated by 13 ms (approximately the duration of one frame in the multifocal sequence). The flash at t_{-1} is preceded by a train of pulses 26 ms apart to simulate the average density of flashes in the multifocal sequence. At t_{-1} and t_0, one of the four possible two-frame sequences occurs. For each sequence, the waveform of the continuous record is shown. The simulated first- and second-order kernels are calculated by combining the four sets of records, exactly as in Fig. 25A.

This simulation is a highly simplified version of both the m-sequence and of the first- and second-order kernels, but the simulated responses (shown in Fig. 26D for ready comparison to the multifocal kernels) capture some of the key aspects of the first- and second- order kernels of the mERG. Like the mERG, the simulated first-order kernel peaks earlier than the traditionally recorded ERG and has less prominent oscillatory components. The simulated second-order kernel in Fig. 26D also bears some resemblance to the second-order mERG (Fig. 26A).

The actual mERG can be more closely approximated by adding other terms.[3] However, the waveforms of the simulated kernels in Fig. 26D are similar enough to the waveforms of the mERG kernels as to illustrate some key aspects of the mERG. First, the two components (RbW and RwW) that make up the first-order kernel are very different in waveform; one is certainly not a scaled-down version of the other. In fact, they are about the same amplitude. Second, there is no actual response that corresponds to the first-order kernel of the mERG. Third, the second-order kernel is the result of a subtraction of two responses and its strange shape reflects the fact that they have different waveforms. The second-order kernel is undoubtedly due to more than one nonlinear process. One process involved is probably a short-term adaptive mechanism that removes some of the oscillatory components and shortens the peak of the positive wave P1 in a manner similar to the action of a steady background (see Fig. 10 in Hood *et al.*, 1997). Fourth, unlike the schematics in Figs. 2 and 25, the responses to successive flashes overlap. Examine the response in the continuous records in Fig. 27 to the flash at t_{-1} (arrows a and b). The response to this flash overlaps the response to the next flash (arrow 2). Alternately, compare the responses to the flashes at t_0 (arrows 1 and 2) with

[3]This simulation, of course, does not consider the other slices of the second-order kernel nor the effects of higher-order kernels. Our simulations show that a particularly important set of conditions involves adding one addition frame at t_{-2} so the response RwwW and RbbW can be considered. Further, this simulation does not consider the effect of the flash that immediately follows.

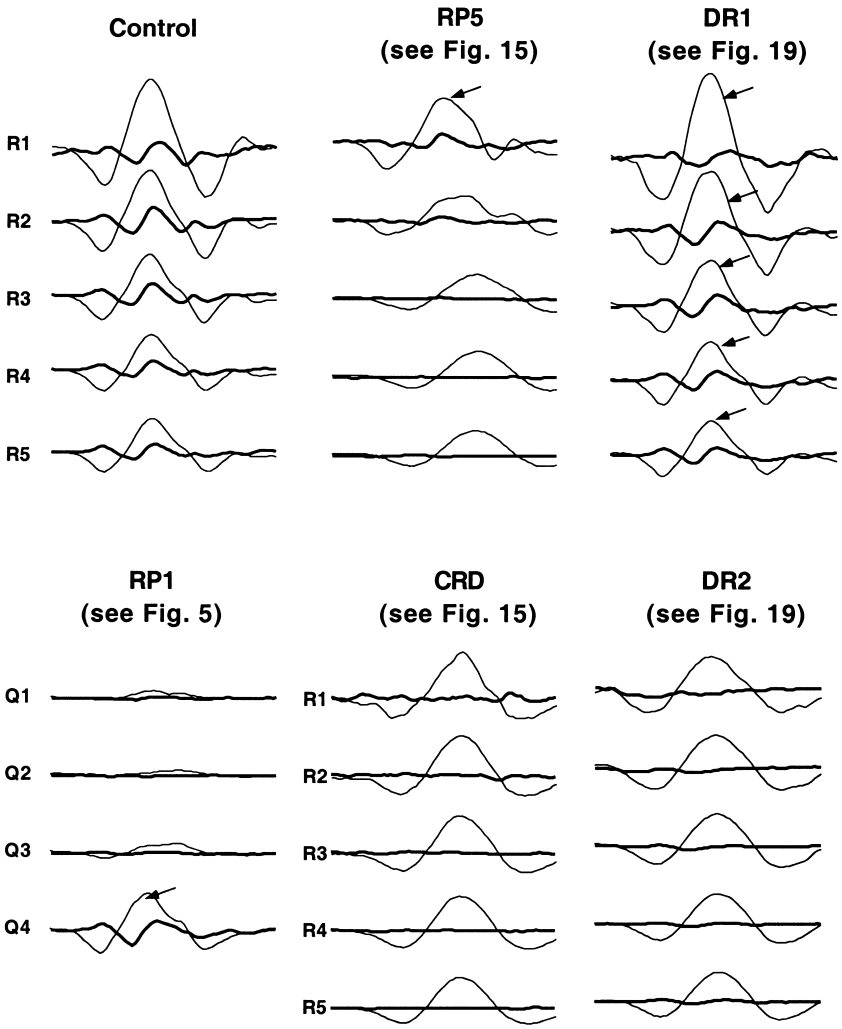

Fig. 28. The first-order (thin curve) and second-order (bold curve) responses were summed by rings as in Fig. 10 for the control subject whose records are in Fig. 6B and for patients RP5, DR1 and DR2, whose records are in Figs. 15 and 19. The first-order (thin curve) and second-order (bold curve) kernels were summed by quadrants as in Fig. 17 for RP1, whose records are in Fig. 5.

and without a preceding flash. Fifth, because the responses overlap, the resulting combined response will often be smaller than the response to a single flash (compare arrows 2 and b). The appearance of a smaller response may be largely due to the addition of two independent responses. Sixth, to the extent that the retina does not process the responses independently, due, for example, to response compression, gain changes or active inhibition, the shape of the first-order kernel will be affected. In general, it should be clear from the analysis above (Figs. 25–27) that the waveform of the first-order kernel is shaped by the responses to a series of flashes both prior and subsequent to the nominally "eliciting" flash (the flash at t_0). Thus, the first-order mERG response (kernel) may be a "little ERG" in the sense that it can be broken into contributions from the same cellular components as the full-field ERG (see Sections 2.4 and 4.3.1 and Hood *et al.*, 1997). However, it is not a "little ERG" that is simply modified by the adapting con-

ditions of the m-sequence, as implied by Hood *et al*. (1997).

Some of the points made in this section have been recently illustrated via a recombination of the individual responses that make up the mERG (Sutter, 2000).

5.6. Implications for the study of retinal disease

5.6.1. *A missing component or an abnormal process*

If a retinal disease eliminated the second-order kernel but not the first-order kernel, what could be said about the site(s) and/or mechanism(s) involved? The answer depends upon a better understanding of the second-order kernel from the normal retina. If the "adapting effect" of the preceding flash removes a retinal component, then a missing second-order kernel implies a missing component. In fact, a diminished second-order kernel has been attributed to a missing inner retinal or optic nerve head component. On the other hand, if an "adaptation process" initiated by the preceding flash modifies the response, then a missing second-order kernel implies an abnormal process. For example, Palmowski *et al*. (1997) found altered second-order kernels in patients with diabetic retinopathy and attributed these alterations to an abnormal adaptation process (gain mechanism) in the inner retina of these patients. Of course, these two possibilities are not mutually exclusive.

5.6.2. *Evidence for an abnormal process*

The analysis in Fig. 28 suggests that the large, but delayed first-order kernels seen in some patients above may be associated with an abnormal adaptation process. Here, the summed mERG responses are shown for rings as in Fig. 10 (note that the center response is not shown in Fig. 28). In the case of RP1, the responses are summed by quadrant as in Fig. 17, since this patient has one essentially normal quadrant (Fig. 5). In all cases, when the first-order kernel is large and abnormally slow, the second-order kernel is missing (non-detectable). When the first-order kernel has normal timing (responses with arrows), the second-order kernel is reasonably large. This distinction even holds within a single patient (e.g. RP5) and for the patient (DR1) who has the mERG responses with normal timing in regions of abnormal field sensitivity. We speculate that the damage in these retinas affects a mechanism that controls the time course of the response. This mechanism, perhaps a time-dependent gain change, would be necessary for the normal timing of the mERG response and would be the source of the waveform changes captured in the second-order kernel. We argued above that these large, substantially delayed responses reflect damage proximal to the photoreceptor outer segment, probably in the outer-plexiform layer. Thus, we can speculate that the abnormal adaptation, which is reflected in the diminished second-order response, is either due to an abnormal mechanism of adaptation in the outer plexiform layer or an abnormal outer plexiform layer response into the cells responsible for adaptation in the inner plexiform layer. In either case, a missing second-order kernel may prove to be a robust marker for damage to the outer-plexiform layer, not the inner plexiform layer as commonly assumed.

6. FUTURE DIRECTIONS

The mERG holds great promise for the study of human retinal function. This is especially true in the case of diseases that affect the cone-driven retina unevenly. However, if the multifocal technique is to realize its promise, then progress must be made on three fronts. First, we need a better understanding of the cellular components of the primate photopic full-field and multifocal ERGs. Here primate research, both chemical isolation of cellular contributions in vivo and intracellular recording of bipolar and amacrine cells in situ, should lead the way. Second, we are only beginning to understand the nonlinear mechanisms that shape the mERG waveform. These nonlinear mechanisms should not be viewed simply in the context of the mERG, but rather as mechanisms more generally involved in retinal function. Here, our growing knowledge of retinal mechanisms of adaptation should be of help. Computational

models of retinal adaptation are being developed (see review by Hood, 1998) and an application of these models to the mERG may be possible in the near future. Third, there is a need for quantitative models to predict and explain the effects of disease. Table 1 is a naïve characterization of what is needed here. We need approaches that combine models of adaptation with models of disease action. As we have seen, adaptation is involved in the mERG paradigm. Thus, any hypothesized action of a disease must specify how the mechanisms of adaptation are affected. [See discussion in Hood (1988) and Hood and Greenstein (1990).] Finally, in the process of filling in the gaps in our knowledge, we can avoid the mistakes of the past by remembering that the cells and mechanisms generating the mERG kernels are the same as those generating the conventional, full-field ERG. Consequently, what we know about the full-field ERG need not be re-learned. The need to worry about the state of the subject's adaptation (Kondo *et al*., 1999), the possible influence of rod intrusion, and the possibility of rod-cone interactions are only some of the many lessons to be learned from earlier work with the full-field ERG.

Acknowledgements—Supported by grants from the National Eye Institute R01-EY-02115 and R01-EY-09076. The author gratefully acknowledges the valuable suggestions made by Dr. Sherif Shady on earlier versions of this manuscript and by Drs. Marc Bearse, Brad Fortune, Laura Frishman, Vivienne Greenstein, Karen Holopigian, Randy Kardon, and Bill Seiple on a final draft. Finally, this review would not exist had it not been for the ingenious work of Erich Sutter in inventing and developing the multifocal technique. The author is grateful for the patient help and warm friendship supplied by both Erich Sutter and Marc Bearse over the last four years.

REFERENCES

Baseler, H. A., Sutter, E. E., Klein, S. A. and Carney, T. (1994) The topography of visual evoked response properties across the visual field. *Electroencephal. Clin. Neurophysiol.* **90**, 65–81.

Bearse, M. A. and Sutter, E. E. (1996) Imaging localized retinal dysfunction with the multifocal electroretinogram. *J. Opt. Soc. Amer.* **13**, 634–640.

Bearse, M. A., Sutter, E. E., Sim, D. and Stamper, R. (1996) Glaucomatous dysfunction revealed in higher order components of the electroretinogram. In *Vision Science and Its Applications*, *OSA Tech Dig. Ser*, 1, pp. 104–107. Optical Society of America, Washington, DC.

Bearse, M. A., Sutter, E. E. and Palmowski, A. M. (1997) New developments toward a clinical test of retinal ganglion cell function. In *Vision Science and Its Applications*, *OSA Tech Dig. Ser*, 1, pp. 280–283. Optical Society of America, Washington, DC.

Bearse, M. A. and Sutter, E. E. (1998) Contrast dependence of multifocal ERG components. In *Vision Science and its Applications*, *Osa Tech. Dig. Ser*, 1, pp. 24–27. Optical Society of America, Washington, DC.

Berson, E. (1993) Retinitis pigmentosa: the Friedenwald lecture. *Invest. Ophthal. Vis. Sci.* **34**, 1659–1676.

Berson, E. L., Gouras, P., Gunkel, R. D. and Myrianthopoulos, N. C. (1969a) Rod and cone responses in sex-linked retinitis pigmentosa. *Arch. Ophthal.* **81**, 215–225.

Berson, E., Gouras, P. and Hoff, M. (1969b) Temporal aspects of the electroretinogram. *Arch. Ophthal.* **81**, 207–214.

Birch, D. G., Hood, D. C., Nusinowitz, S. and Pepperberg, D. R. (1995) Abnormal activation and inactivation mechanisms of rod transduction in patients with autosomal dominant retinitis pigmentosa and the pro-23-his mutation. *Invest. Ophthal. Vis. Sci.* **36**, 1603–1614.

Bush, R. A. and Sieving, P. (1994) A proximal retinal component in the primate photopic ERG a-wave. *Invest. Ophthal. Vis. Sci.* **35**, 635–644.

Chan, H. L. and Brown, B. (1998) Investigation of retinitis pigmentosa using the multifocal electroretinogram. *Ophthal. Physiol. Opt.* **18**, 335–350.

Chan, H. L. and Brown, B. (1999) Multifocal ERG changes in glaucoma. *Ophthal. Physiol. Opt.* **19**, 306–316.

Curcio, C. A., Sloan, K. R., Kalina, R. E. and Hendrickson, A. E. (1990) Human photoreceptor topography. *J. Comp. Neurol.* **292**, 497–523.

Felius, J. and Swanson, W. H. (1999) Photopic temporal processing in retinitis pigmentosa. *Invest. Ophthal. Vis. Sci.* **40**, 2932–2944.

Fortune, B., Schneck, M. E. and Adams, A. J. (1999) Multifocal electroretinogram delays reveal local retinal dysfunction in early diabetic retinopathy. *Invest. Ophthal. Vis. Sci.* **40**, 2638–2651.

Fortune, B., Cioffi, G. A., Johnson, C. A., Kondo, Y., Mochizuki, K. and Kitazwa, Y. (2000). The relationship between multifocal electroretinogram and standard automated perimetry findings in normal tension glaucoma. in press.

Frishman, L. J., Shen, F. F., Du, L., Robson, J. G., Harwerth, R. S., Smith, E. L. III, Carter-Dawson, L. and Crawford, M. L. J. (1996) The scotopic electroretinogram of macaque after retinal ganglion cell loss from experimental glaucoma. *Invest. Ophthal. Vis. Sci.* **37**, 125–141.

Frishman, L. J., Hood, D. C., Saszik, S., Viswanathan, S. and Robson, J. G. (2000a) Outer retinal contributions to the *macaque's* multifocal ERG, in preparation.

Frishman, L. J., Saszik, S., Harwerth, R. S., Viswanathan, S., Li, Y., Smith, E. L., Robson, J. G. and Barnes, G. (2000b) Effects of experimental galucoma in macaques on the multifocal ERG. *Doc. Ophthal.*, in press.

Graham, S. L., Klistorner, A. I., Grigg, J. R. and Billson, F. A. (2000) Objective VEP perimetry in glaucoma: asymmetry analysis to identify early defects. *J. Glau.* **9**, 10–19.

Granit, R. (1947) *Sensory Mechanism of the Retina*. Oxford University Press, London.

Greenstein, V. C., Holopigian, K., Hood, D. C., Seiple, W. and Carr, R.E. (2000) The nature and extent of retinal dysfunction associated with diabetic macular edema. *Invest. Ophthal. Vis. Sci.*, in press.

Hare, W., Ton, H., Woldemussie, E., Ruiz, G., Feldmann, B. and Wijono, M. (1999) Electrophysiological and histological measures of retinal injury in chronic ocular hypertensive monkeys. *Eur. J. Ophthal.* **9**(Suppl 1), 30–33.

Hasegawa, S., Takagi, M., Usui, T., Takada, R. and Abe, H. (2000) Waveform changes of the first-order multifocal electroretinogram in patients with glaucoma. *Invest. Ophthal. Vis. Sci.* **41**, 1597–1603.

Holopigian, K., Seiple, W., Greenstein, V. C., Hood, D. C., Wladis, E. J. and Carr, R. E. (1998) Localized rod and cone ERG responses in patients with RP and cone dystrophy. *Invest. Ophthal. Vis. Sci.* **39**, S969.

Hood, D. C. (1988) Testing hypotheses about development with ERG and incremental threshold data. *J. Opt. Soc. Amer.* **5**, 2159–2165.

Hood, D. C. (1998) Lower-level visual processing and models of light adaptation. *Ann. Rev. Psychol.* **49**, 503–535.

Hood, D. C. and Birch, D. G. (1995) Abnormal cone receptor activity in patients with hereditary degeneration. In *Degenerative Diseases of the Retina* (eds. R. E. Anderson *et al.*) pp. 349–358. Springer, Berlin.

Hood, D. C. and Birch, D. G. (1996a) The b-wave of the scotopic (rod) ERG as a measure of the activity of human on-bipolar cells. *J. Opt. Soc. Amer.* **13**, 623–633.

Hood, D. C. and Birch, D. G. (1996b) Abnormalities of the retinal cone system in retinitis pigmentosa. *Vis. Res.* **36**, 1699–1709.

Hood, D. C. and Birch, D. G. (1997) Assessing abnormal rod photoreceptor activity with the a-wave of the ERG: applications and methods. *Doc. Ophthal.* **92**, 253–267.

Hood, D. C. and Greenstein, V. C. (1990) Models of the normal and abnormal rod system. *Vis. Res.* **30**, 51–68.

Hood, D. C. and Li, J. (1997) A technique for measuring individual multifocal ERG records. In *Non-invasive Assessment of the Visual System, Trends in Optics and Photonics*, vol. 11 (ed. D. Yager) pp. 33–41. Optical Society of America, Washington, DC.

Hood, D. C., Seiple, W., Holopigian, K. and Greenstein, V. C. (1997) A comparison of the components of the multi-focal and full-field ERGs. *Vis. Neurosci.* **14**, 533–544.

Hood, D. C., Zhang, X. (2000) Multifocal ERG and VEP responses and visual fields: comparing disease-related changes. *Doc. Ophthal.*, in press.

Hood, D. C., Holopigian, K., Seiple, W., Greenstein, V., Li, J., Sutter, E. E. and Carr, R. E. (1998a) Assessment of local retinal function in patients with retinitis pigmentosa using the multi-focal ERG technique. *Vis. Res.* **38**, 163–179.

Hood, D. C., Wladis, E. J., Shady, S., Holopigian, K., Li, J. and Seiple, W. (1998b) Multifocal rod electroretinograms. *Invest. Ophthal. Vis. Sci.* **39**, 1152–1162.

Hood, D. C., Greenstein, V., Frishman, L., Holopigian, K., Viswanathan, S., Seiple, W., Ahmed, J. and Robson, J. G. (1999a) Identifying inner retinal contributions to the human multifocal ERG. *Vis. Res.* **39**, 2285–2291.

Hood, D. C., Frishman, L. J., Robson, J. G., Shady, S., Ahmed, J. and Viswanathan, S. (1999b) A frequency analysis of the regional variation in the contribution from action potentials to the primate multifocal ERG. In *Vision Science and Its Applications*, *OSA Tech. Dig. Ser.*, 1, pp. 56–59. Optical Society of America, Washington, DC.

Hood, D. C., Frishman, L. J., Viswanathan, S., Robson, J. G. and Ahmed, J. (1999c) Evidence for a ganglion cell contribution to the primate electroretinogram (ERG): effects of TTX on the multifocal ERG in macaque. *Vis. Neurosci.* **16**, 411–416.

Hood, D. C., Frishman, L. J., Saszik, S., Viswanathan, S. and Robson, J. G. (2000a) The variations in the waveform of the primate cone ERG with retinal eccentricity depend upon inner and outer retinal contributions. *Invest. Ophthal. Vis. Sci.* **41**(suppl), S496.

Hood, D. C., Greenstein, V. C., Holopigian, K., Bauer, R., Firoz, B., Liebmann, J. M., Odel, J. G. and Ritch, R. (2000b) An attempt to detect glaucomatous damage to the inner retina with the multifocal ERG. *Invest. Ophthal. Vis. Sci.* **41**, 1570–1579.

Hood, D. C., Zhang, X., Greenstein, V. C., Kangovi, S., Odel, J. G., Liebman, J. M. and Ritch, R. (2000c) An interocular comparison of the multifocal VEP: a possible technique for detecting local damage to the optic nerve. *Invest. Ophthal. Vis. Sci.* **41**, 1580–1587.

Horiguchi, M., Suzuki, S., Kondo, M., Tanikawa, A. and Miyake, Y. (1998) Effect of glutamate analogues and inhibitory neurotransmitters on the electroretinograms elicited by random sequence stimuli in rabbits. *Invest. Ophthal. Vis. Sci.* **39**, 2171–2176.

Keating, D., Parks, S., Evans, A. L., Williamson, T. H., Elliott, A. T. and Jay, J. L. (1997) The effect of filter bandwidth on the multifocal electroretinogram. *Doc. Ophthal.* **92**, 291–300.

Keating, D., Parks, S. and Evans, A. L. (2000) Technical aspects of multifocal ERG recording. *Doc. Ophthal.*, in press.

Klistorner, A. I., Graham, S. L., Grigg, J. R. and Billson, F. A. (1998) Multifocal topographic visual evoked potential: improving objective detection of local visual field defects. *Invest. Ophthal. Vis. Sci.* **39**, 937–950.

Kondo, M., Miyake, Y., Horiguchi, M., Suzuki, S. and Tanikawa, A. (1995) Clinical evaluation of multifocal electroretinogram. *Invest. Ophthal. Vis. Sci.* **36**, 2146–2150.

Kondo, M., Miyake, Y., Piao, C., Tanikawa, A., Horiguchi, M. and Terasaki, H. (1999) Amplitude increase of the multifocal electroretinogram during light adaptation. *Invest. Ophthal. Vis. Sci.* **40**, 2633–2637.

Kretschmann, U., Seeliger, M. W., Ruether, K., Usui, T., Apfelstedt-Sylla, E. and Zrenner, E. (1998a) Multifocal electroretinography in patients with Stargardt's macular dystrophy. *Brit. J. Ophthal.* **82**, 267–275.

Kretschmann, U., Seeliger, M., Ruether, K., Usui, T. and Zrenner, E. (1998b) Spatial cone activity distribution in diseases of the posterior pole determined by multifocal electroretinography. *Vis. Res.* **38**, 3817–3828.

Massey, S. C. and Maguire, G. (1995) The role of glutamate in retinal circuitry. In *Excitatory Amino Acids and Synaptic Transmission* (eds. H. V. Wheal and A. M. Thomson) pp. 201–221. Academic Press, San Diego, CA.

Miyake, Y., Shiroyama, N., Horiguchi, M. and Ota, I. (1989) Asymmetry of focal ERG in human macular region. *Invest. Ophthal. Vis. Sci.* **30**, 1743–1749.

Miyake, Y. (1990) Macular oscillatory potentials in humans. *Doc. Ophthal.* **75**, 111–124.

Miyake, Y., Horiguchi, M., Tomita, N., Kondo, M., Tanikawa, A., Takahashi, H., Suzuki, S. and Terasaki, H. (1996) Occult macular dystrophy. *Amer. J. Ophthal.* **122**, 644–653.

Mizener, J. B., Kimura, A. E., Adamus, G., Thirkill, C. E., Goeken, J. A. and Kardon, R. H. (1997) Autoimmune retinopathy in the absence of cancer. *Amer. J. Ophthal.* **123**, 607–618.

Moore, P. A., Sonkin, P., Oh, K. T., Boldt, H. C. and Kardon, R. H. (1999) Recovery of the multifocal electroretinogram (mERG) and visual field in macular-off retinal detachment. *Invest. Ophthal. Vis. Sci.* **40**(Suppl), S19.

Nagatomo, A., Nao-i, N., Mariuiwa, F., Arai, M. and Sawada, A. (1998) Multifocal electroretinograms in normal subjects. *Jpn. J. Ophthal.* **42**, 129–135.

Odel, J., Holopigian, K. and Hood, D. C. (1999) Multifocal ERG and threshold perimetry in occult macular dystrophy. *Invest. Ophthal. Vis. Sci.* **40**(Suppl), S715.

Palmowski, A. M., Sutter, E. E., Bearse, M. A. and Fung, W. (1997) Mapping of retinal function in diabetic retinopathy using the multifocal electroretinogram. *Invest. Ophthal. Vis. Sci.* **38**, 2586–2596.

Parks, S., Keating, D., Evans, A. L., Williamson, T. H., Jay, J. L. and Elliot, A. T. (1997) *Doc. Ophthal.* **92**, 281–289.

Radtke, N. D., Aramant, R. B., Seiler, M. and Petry, H. M. (1999) Preliminary report: indications of improved visual function after retinal sheet transplantation in retinitis pigmentosa patients. *Amer. J. Ophthal.* **128**, 384–387.

Riggs, L. A. (1965) Electrophysiology of vision. In *Vision and Vision Perception* (ed. C. H. Graham) pp. 81–131. Wiley, New York.

Ripps, H., Noble, K. G., Greenstein, V. C., Siegel, I. M. and Carr, R. E. (1987) Progressive cone dystrophy. *Ophthal.* **94**, 1401–1409.

Robson, J. G. and Frishman, L. J. (1999) Dissecting the dark-adapted electroretinogram. *Doc. Ophthal.* **95**, 187–215.

Sasoh, M., Yoshida, S., Kuze, M. and Uji, Y. (1998) The multifocal electroretinogram in retinal detachment. *Doc. Ophthal.* **94**, 239–252.

Seeliger, M. W., Kretschmann, U. H., Apfelstedt-Sylla, E. and Zrenner, E. (1998a) Implicit time topography of multifocal electroretinograms. *Invest. Ophthal. Vis. Sci.* **39**, 718–723.

Si, Y.-J., Kishi, S. and Aoyagi, K. (1999) Assessment of macular function by multifocal electroretinogram before and after macular hole surgery. *Brit. J. Ophthal.* **83**, 420–424.

Seeliger, M., Kretschmann, U., Apfelstedt-Sylla, E., Ruther, K. and Zrenner, E. (1998b) Multifocal electroretinography in retinitis pigmentosa. *Amer. J. Ophthal.* **125**, 214–226.

Sieving, P. A., Murayama, K. and Naarendorp, F. (1994) Push-pull model of the primate photopic electroretinogram: a role for hyperpolarizing neurons in shaping the b-wave. *Vis. Neurosci.* **11**, 519–532.

Stafford, D. K. and Dacey, D. M. (1997) Physiology of the A1 amacrine: a spiking, axon-bearing interneuron of the macaque monkey retina. *Vis. Neurosci.* **14**, 507–522.

Sutter, E. E. (1991) The fast m-transform: a fast computation of cross-correlations with binary m-sequences. *Soc. Ind. Appl. Math.* **20**, 686–694.

Sutter, E. E. (2000) The interpretation of multifocal binary kernels. *Doc. Ophthal.*, in press.

Sutter, E. E. and Tran, D. (1992) The field topography of ERG components in man-I. The photopic luminance response. *Vis. Res.* **32**, 433–466.

Sutter, E. E. and Bearse, M. A. (1995) Extraction of a ganglion cell component from the corneal response. In *Vision Science and its Applications*, *OSA Tech. Dig. Ser.*, 1, pp. 310–313. Optical Society of America, Washington, DC.

Sutter, E. E. and Bearse, M. A. (1998) The retinal topography of local and lateral gain control mechanisms. In *Vision Science and its Applications*, *OSA Tech. Dig. Ser.*, 1, pp. 20–23. Optical Society of America, Washington, DC.

Sutter, E. E. and Bearse, M. A. (1999) The optic nerve head component of the human ERG. *Vis. Res.* **39**, 419–436.

Sutter, E. E., Shimada, Y., Li, Y. and Bearse, M. A. (1999) Mapping inner retinal function through enhancement of adaptive components in the m-ERG. In *OSA Tech Dig. Ser.*, *Vision Science and its Applications*, 1, pp. 52–55. Optical Society of America, Washington, DC.

Vaegan and Buckland, L. (1996) The spatial distribution of ERG losses across the posterior pole of glaucomatous eyes in multifocal recordings. *Aust. NZ J. Ophthal.* **14**(Suppl 2), 28–31.

Vaegan and Sanderson, G. (1997) Absence of ganglion cell subcomponents in multifocal luminance electroretinograms. *Aust. NZ J. Ophthal.* **25**(Suppl 1), S87–90.

Verdon, W. A. and Haegerstrom-Portnoy, G. (1998) Topography of the multifocal electroretinogram. *Doc. Ophthal.* **95**, 73–90.

Viswanathan, S., Frishman, L. J., Robson, J. G., Harwerth, R. S. and Smith III, E. L. (1999) The photopic negative response of the macaque electroretinogram is reduced by experimental glaucoma. *Invest. Ophthal. Vis. Sci.* **40**, 1124–1136.

Viswanathan, S. Frishman, L. J., Robson, J. G. (2000) The uniform field and pattern ERG in macaques with experimental glaucoma. *Invest. Ophthal. Vis. Sci.*, in press.

Wu, S. and Sutter, E. E. (1995) A topographic study of oscillatory potentials in man. *Vis. Neurosci.* **12**, 1013–1025.

Yoshii, M., Murakami, A., Akeo, K., Fujiki, K., Saga, M., Mizukawa, A., Itoh, J., Okisaka, S., Yanashima, K. and Hotta, Y. (1998) Visual function in retinitis pigmentosa related to a codon 15 rhodopsin gene mutation. *Ophthal. Res.* **30**, 1–10.